Cytomegalovirus infection of the fetal brain: intake of aspirin during pregnancy blunts neurodevelopmental pathogenesis in the offspring

Sarah Tarhini, Carla Crespo-Quiles, Emmanuelle Buhler, Louison Pineau, Emilie Pallesi-Pocachard, Solène Villain, Saswati Saha, Lucas Silvagnoli, Thomas Stamminger, Hervé Luche, et al.

Journal of Neuroinflammation

RESEARCH

Open Access

Cytomegalovirus infection of the fetal brain: intake of aspirin during pregnancy blunts neurodevelopmental pathogenesis in the offspring

Sarah Tarhini[1], Carla Crespo-Quiles[1,6], Emmanuelle Buhler[1], Louison Pineau[1,7], Emilie Pallesi-Pocachard[1], Solène Villain[1], Saswati Saha[2,8], Lucas Silvagnoli[1], Thomas Stamminger[3], Hervé Luche[4], Carlos Cardoso[1], Jean-Paul Pais de Barros[5], Nail Burnashev[1], Pierre Szepetowski[1*] and Sylvian Bauer[1*]

Abstract

Background Congenital cytomegalovirus (CMV) infections represent one leading cause of human neurodevelopmental disorders. Despite their high prevalence and severity, no satisfactory therapy is available and pathophysiology remains elusive. The pathogenic involvement of immune processes occurring in infected developing brains has been increasingly documented. Here, we have used our previously validated rat model of CMV infection of the fetal brain in utero to test whether the maternal administration of four different drugs with immunomodulatory properties would have an impact on the detrimental postnatal outcome of CMV infection.

Methods CMV infection of the rat fetal brain was done intracerebroventricularly. Each of the drugs, including acetylsalicylic acid (aspirin, ASA), a classical inhibitor of cyclooxygenases Cox-1 and Cox-2, the two key rate-limiting enzymes of the arachidonic acid-to-prostaglandins (PG) synthesis pathway, was administered to pregnant dams until delivery. ASA was selected for subsequent analyses based on the improvement in postnatal survival. A combination of qRT-PCR, mass spectrometry-based targeted lipidomics, immunohistochemistry experiments, monitoring of neurologic phenotypes and electrophysiological recordings was used to assess the impact of ASA in CMV-infected samples and pups. The postnatal consequences of CMV infection were also analyzed in rats knocked-out (KO) for Cox-1.

Results Increased PGE2 levels and increased proportions of Cox-1^+ and Cox-2^+ microglia were detected in CMV-infected developing brains. Maternal intake of ASA led to decreased proportion of Cox-1^+ fetal, but not neonatal, microglia, while leaving the proportions of Cox-2^+ microglia unchanged. Maternal intake of ASA also improved the key postnatal in vivo phenotypes caused by CMV infection and dramatically prevented against the spontaneous epileptiform activity recorded in neocortical slices from CMV-infected pups. In contrast with maternal intake of ASA, Cox-1 KO pups displayed no improvement in the in vivo phenotypes after CMV infection. However, as with ASA

*Correspondence:
Pierre Szepetowski
pierre.szepetowski@inserm.fr
Sylvian Bauer
sylvian.bauer@inserm.fr
Full list of author information is available at the end of the article

administration, the spontaneous epileptiform activity was dramatically inhibited in neocortical slices from CMV-infected, Cox-1 KO pups.

Conclusion Overall, our data indicate that, in the context of CMV infection of the fetal brain, maternal intake of ASA during pregnancy improved CMV-related neurodevelopmental alterations in the offspring, likely via both Cox-1 dependent and Cox-1 independent mechanisms, and provide proof-of-principle for the use of ASA against the detrimental outcomes of congenital CMV infections.

Keywords CMV, Herpes virus, Fetal brain, Lipids, Cox-1, Cyclooxygenase

Background

Neurodevelopment may be altered by numerous genetic defects and by environmental factors. These latter include congenital infections by pathogens such as zika virus or cytomegalovirus (CMV). Congenital CMV infections are one leading cause of human neurodevelopmental disorders. Indeed, they represent about 1% of all live births worldwide [1–3]. While 80–85% of CMV-infected neonates are considered unaffected, the other 15–20% are born with, or will develop, severe neurologic disorders and other defects, including increased neonatal lethality, growth retardation, brain malformations (e.g. polymicrogyria), hearing loss, vision impairment, cerebral palsy, epileptic seizures, and intellectual disability. Furthermore, a more long-term influence of congenital CMV infection on common brain diseases such as autism disorders or schizophrenia has been proposed [2, 4]. While congenital CMV is of crucial public health and medical importance, no satisfactory preventive or curative therapy is available and the underlying neuropathogenesis remains poorly understood.

Analyses of CMV-infected human fetal brains have revealed CMV infection in different regions of the brain, notably the periventricular areas, and also the hippocampus, the cerebellum, the brain stem, the amygdala, the thalamus, the basal ganglia, the olfactory bulbs, and the neocortex, with quite equal distribution in the frontal, temporal, parietal and occipital lobes [5]. The infected brains showed mild to severe inflammatory lesions that included focal necrosis, microglia nodules and activated microglia [6–8]. Interestingly, a correlation between high levels and broad distribution of innate immune cells in the infected brains, and the severity of the brain lesions was found [7]. Generally, brain immune processes have been increasingly recognized as important actors in brain development and pathology [9]. In the recent years, studies in relevant rodent models of CMV infection and, as stated above, analyses of CMV-infected human brain samples, have yielded convergent insights into the alteration and the possible participation of various innate and adaptive immune responses in the related developmental neuropathogenesis [7, 10–21]. Various immunomodulatory strategies have been used in different rodent models of CMV infection, including the adoptive transfer of CMV-specific $CD8^+$ T cells [12], the use of tumor necrosis factor alpha-neutralizing antibodies [17], or the administration of glucocorticoids [13]. In a rat model of CMV infection of the developing brain in utero characterized by early brain immune alterations [20], the targeting of altered fetal microglia, either via acute injection of clodronate liposomes in the fetal brain to transiently deplete microglia, or via chronic administration to the dam throughout pregnancy of doxycycline, an antibiotic with immunomodulatory activity, led to dramatic improvements of the various postnatal phenotypes that were caused by CMV infection of the rat fetal brain, *i.e.* decreased survival and weight gain, impaired sensorimotor development, hindlimb hyperextension, and generalized tonic–clonic epileptic seizures (GTCS) [21].

In the present study, we have tested a novel series of drugs with immunomodulatory effects and selected based on their previously reported impacts on microglia. Vitamin C was shown to prevent against microglia activation, which in turn could be triggered by inhibiting the sodium-vitamin C cotransporter 2 [22]. N-acetyl-L-cysteine (NAC) was chosen as a well-known anti-inflammatory agent which acted against reactive microglia in animal models of cerebral palsy [23] and of necrotizing enterocolitis-associated brain injury [24]. Acetylsalicylic acid (aspirin, ASA) was selected as it inactivates cyclooxygenases Cox-1 (also known as PG-endoperoxide synthase 1, Ptgs1) and Cox-2 (Ptgs2) [25] that are key, rate-limiting enzymes of the arachidonic acid-to-prostaglandins (PGs) synthesis pathway (PG pathway). PGs are lipid molecules that are produced in physiological conditions and in response to various stimuli; they participate in critical phases of inflammation following insults of the immature brain [26]. It was shown that Cox enzymes and the downstream effector PGE2 receptor influence microglia [27, 28]. Last, prednisolone was used not only as it is a classical anti-inflammatory compound with immunosuppressant effects, but also as glucocorticoids influence microglia function [29] and have been previously administered to CMV-infected

newborn mice [13]. The possible beneficial effect of either of these four drugs administered during pregnancy was assessed in our previously validated rat model of CMV infection of the fetal brain in utero [20, 21].

Material and methods

Ethical statement

Animal experimentations were performed in accordance with the French legislation and in compliance with the European Communities Council Directives (2010/63/UE). This study was approved under the French department of agriculture and the local veterinary authorities by the Animal Experimentation Ethics Committee (Comité d'Ethique en Expérimentation Animale) n°014 under licences n°01010.02, n°7256-2016100715494790 v3 and n°40278-202212051629511 v6.

CMV infection and pharmacological treatments

Naive timed pregnant Wistar rats were obtained at Charles River & Janvier Labs, France. Cox-1 KO (HsdSage:SD-Cox1tm1Sage) Sprague–Dawley rats originally created and validated at SAGE Labs, Inc. (St Louis, MO, USA) were purchased and cryorecovered at Envigo (St Louis, MO, USA). Cox-1 heterozygous males and females were mated in order to generate litters with a mix of homozygous, heterozygous and wild-type pups. Cox-1 alleles were detected by PCR using the following primer pairs: Cox1-F2: 5′-gctctctcatgtgtcatcgct, Cox-1-R3: 5′-tctcggatgaaggtggcattc, and Cox1-cel1-F: 5′-attttgggtcctggctctct, Cox1-cel1-R: 5′-cttgctttatgtggcaacca. All animals were raised at INMED animal facility and kept at room temperature under conditions of optimal health and hygiene. Rat cytomegalovirus (rat CMV) recombinant Maastricht strain (RCMV-Δ145–147-gfp) with a green fluorescent protein (GFP) expression cassette, and its production, purification and titration, were reported and done as previously [20, 30]. In utero intracerebroventricular (icv) injections were performed according to previously reported studies [20, 21] in embryos from timed pregnant rats (embryonic Day 15, E15) that were anaesthetized with isoflurane (4% for induction, then 2.5%). Briefly, 1 µL of minimal essential medium (MEM) with FastGreen (2 mg/mL; Sigma-Aldrich, Saint-Quentin Fallavier, France), either containing 3.5×10^3 plaque forming unit (pfu) of rat CMV, or not (control), was injected icv in each embryo via pulled glass capillaries and a microinjector (PV 820 Pneumatic PicoPump, World Precision Instruments, Friedberg, Germany). In order to target the microglia lineage as soon as from its early generation in the yolk sac [31], drugs were administered in drinking water to the pregnant dams from E5-E6 until delivery, as follows (doses in mg/kg of body weight/day, according to previously reported protocols): vitamin C (L-ascorbic acid; Sigma-Aldrich, 115.8 ± 7.9) [32]; N-acetyl-L-cysteine (NAC; Sigma-Aldrich, 885.4 ± 28.8) [33, 34]; prednisolone (Sigma-Aldrich, 42.5 ± 2.3) [13, 35]; acetylsalicylic acid (aspirin, ASA; Sigma-Aldrich, 66.3 ± 2.5) [36], [37].

Quantitative reverse transcription polymerase chain reaction (qRT-PCR)

Total RNAs were extracted from whole CMV-infected brains at P1 using TRIzol reagent according to manufacturer's instructions (Invitrogen, Thermo Fisher Scientific, Illkirch-Graffenstaden, France). cDNA was synthesized from 1 µg of total RNA using Quantitect Reverse Transcription Kit and according to manufacturer protocol (Qiagen, Courtaboeuf, France). RT-PCRs were then carried out using SYBR-Green chemistry (Roche Diagnostics, Meylan, France) and Roche amplification technology (Light Cycler 480). PCR primers were designed for *Ptgs1* (forward: 5′-ttctgccctctgtacccaaa; reverse: 5′-ggccagaagatgaatatctggta), *Ptgs2* (forward: 5′-cacaaatatgatgttcgcattct; reverse: 5′-ccgtaaacatgatttaagtccactc) and for control gene *Rpl-19* (forward: 5′-ccaaggaagcacgaaagc; reverse: 5′-cctccttggacagagtcttga) for relative quantification. Primer pairs were optimized to ensure specific amplification of the PCR product and the absence of any primer dimer. Quantitative PCR standard curves were set up for all primer pairs. Values of fold change represent averages from triplicate measurements for each sample.

Targeted lipidomics

Embryonic brains (60–90 mg) or postnatal brains (270–312 mg) were extracted and immediately put in 1 mL of methanol/water (80%/20%), then spiked with an internal standard mix containing 13(S)HODE-d4, 9(S)HODE-d4, 15(S)HETE-d8 and PGE2-d4 (1 ng of each in 10 µL) and crushed in an Omni Bead Ruptor 24 apparatus (Omni International, Kennesaw, USA) and circa ten 1.4 mm OD zirconium oxide beads (S = 6.95 m/s, T = 30 s, C = 3; D = 10 s). Lipids were then further extracted by solid phase extraction as described [38]. Lipids (4 µL) were injected on a 1290 HPLC system (Agilent Technologies, Les Ulis, France) equipped with a Zorbax Eclipse SB-C18 (2.1 × 50 mm, 1.8 µm) column maintained at 40 °C. Separation was achieved at a flow rate of 350 µL/min with a linear gradient of water containing 0.1% of acetic acid (A) and methanol containing 0.1% of acetic acid (B) as follows: 55% of A to 15% of A in 10 min then decreased to 2% of A in 8 min and finally maintained at 2% during 2 min. The column was rinsed for 5 min with 55% of A before the next injection. Liquid chromatography

coupled to tandem mass spectrometry (LC–MS/MS) quality grade solvents were purchased from Fischer Scientific (Illkirch-Graffenstaden, France). All other chemicals of the highest grade available were purchased from Sigma-Aldrich.

Acquisition was performed on a 6490 QqQ mass spectrometer operating in negative Single Reaction Monitoring (SRM) mode (source temperature 150 °C, nebulizer 20 L/min, gas flow rate 20 L/min, sheath gas flow 10 L/min, temperature 400 °C, capillary 2500 V, cell acceleration voltage 1 V, collision energy 18 V, 10 V, 16 V and 12 V for HODEs, HETEs, PGE2 and TxB2 respectively). Transitions used for quantitation are given in Figure S2.

Lipid standards 13(S)-hydroxy-9Z,11E-octadecadienoic-9,10,12,13-d4 acid (13(S)-HODE-d4), 9S-hydroxy-10E, 12Z-octadecadienoic-9,10,12,13-d4 acid (9(S)HODE-d4), 15(S)-hydroxy-5Z,8Z,11Z,13E-eicosatetraenoic-5,6,8,9,11, 12,14,15-d8 acid (15(S)HETE-d8) and prostaglandin E2-d4 (PGE2-d4) were purchased from Cayman Chemical (Bertin Pharma, Montigny le Bretonneux, France). 13(S) HODE-d4 and 9(S)HODE-d4 were used for quantification of their undeuterated counterpart. 15(S)HETE-d8 was used for quantitation of HETEs and PGE2-d4 was used for quantification of TxB2 and PGE2. Each lipid species was semi quantitated by calculating their response ratio with regard to the proper internal standards as previously mentioned.

Immunohistochemistry experiments

Immunohistochemistry experiments were carried out on coronal brain slices (80–100 µm, vibratome, Leica) from MEM, CMV and CMV + ASA rat embryos (E17) or rat pups (P1). Briefly, after 1-h incubation at room temperature (RT) in blocking buffer (PBS pH 7.2, 0.5% Triton X-100, 2% serum), sections were incubated at 4 °C with rabbit anti-Iba1 antibody (1:500, Wako, Sobioda, Montbonnot-Saint-Martin, France) and either of mouse anti-Cox-1 (1:400, Cayman Chemical, Interchim, Montluçon, France) or anti-Cox-2 (1:400, Santa Cruz Biotechnology, Heidelberg, Germany) antibody diluted in blocking buffer during 40 h (anti-Cox-1) or 16 h (anti-Cox-2). Slices were then washed and secondary antibodies (goat anti-mouse IgG Alexa-Fluor (AF) 568 for Cox-1, goat anti-mouse IgM AF568 for Cox-2, 1:500; goat anti-rabbit AF633, 1:500, Invitrogen, Thermo Fisher Scientific), diluted in the blocking buffer with 10% serum, were applied for 1h30min at RT. Slices were washed again, stained with Hoechst 33,258 (1:1000, Sigma-Aldrich), and mounted on glass slides using Fluoromount-G Mounting Medium (Invitrogen, Thermo Fisher Scientific).

Microscopy, cell counting and image analyses

Images of brain slices were obtained with a confocal microscope (Zeiss LSM 800) and analyzed according to previously reported procedure [20]. For cell counting, images (2048 × 2048 pixels) were composed of four channels corresponding to Hoechst (460 nm, blue), GFP (488 nm, green), Cox-1 or Cox-2 (568 nm, red), and Iba1 (633 nm, infrared). About 25 stacks of images per section were staggered every 1.5 µm in the z-axis using the 20 × objective. The ipsi and contralateral sides of each section were observed in the periventricular areas (lateral ventricles). Fiji software [39] was used to manually count in each brain the number of $Iba1^+$, $Cox\text{-}1^+$ and of $Iba1^+$, $Cox\text{-}2^+$ cells, as well as the total number of $Iba1^+$ cells. The area of tissue was also measured and was used to compute the densities of total $Iba1^+$ cells per section analyzed. A ratio (percentage) of colocalized cells amongst the total $Iba1^+$ cells was also calculated for each analyzed brain section. Coronal brain sections were selected according to their coordinates as indicated in rat embryonic [40] and neonatal [41] brain atlases. For quantification of the GFP-fluorescent area, images were acquired using a fluorescent stereo microscope (Olympus SZX16) equipped with a digital camera DP73 and were analyzed using Fiji software.

Phenotyping of pups

All phenotypes were evaluated on a daily basis as from P1 during the two first postnatal weeks, as previously reported [21], except the acquisition of the developmental cliff aversion reflex, which was monitored as from P4. Hindlimb hyperextension was detected visually in pups that had a postural misplacement and immobility of their hindlimbs. Generalized tonic–clonic epileptic seizures (GTCS) were detected visually, usually after animal handling, especially during cage changing and behavioral testing.

Extracellular electrophysiological recordings

For slices preparation, brains were rapidly removed from rat pups euthanized after isoflurane (3–4%) anesthesia and placed in an ice-cold slicing solution containing (in mM): 126 choline chloride, 2.5KCl, 1.25 NaH_2PO_4, 7 $MgCl_2$, 0.5 $CaCl_2$, 26 $NaHCO_3$, 10 D-glucose, bubbled with 95% O_2/5% CO_2. 300 µm-thick coronal neocortical slices (Vibratom Leica VT1000S, Leica Microsystems Inc., USA) were left to recover in artificial cerebrospinal fluid solution (ACSF) containing (in mM): 125 NaCl, 3.5 KCl, 1 $CaCl_2$, 2 $MgCl_2$, 1.25 NaH_2PO_4, 26 $NaHCO_3$ and 10 glucose, equilibrated at pH 7.3 with 95% O_2 and 5% CO_2 at 33 °C for about 30 min, then at room temperature (22–25 °C) for about an hour. The final osmolarity of the ACSF solution was 300 ± 5 mOsm.

Slices were then transferred to the recording chamber and perfused with oxygenated ACSF recording solution at 3 mL min^{-1} at 35 °C under a Leica DMLFS microscope (Leica Microsystems Inc., USA). Electrophysiological extracellular recordings of spontaneous local field potentials were obtained from layer IV of the neocortex using a coated nichrome electrode (California Fine Wire, Grover Beach, CA, USA) with a low-noise multichannel DAM-80A amplifier (WPI, UK; high-pass filter 3 Hz; low-pass filter 1 kHz; gain × 1000). Data was digitized using a Digidata 1322A and recorded using Axoscope (Molecular Devices, CA, USA). Recordings were filtered with a low pass 500 Hz filter for analysis using Clampfit software (Molecular Devices, USA). Spikes' frequency was estimated using the threshold event detection with threshold set as twice the background noise.

Use of published RNA sequencing (RNAseq) dataset

Single cell RNAseq data from the developing (E10 to P4) mouse cerebral cortex [42] was obtained from the Broad Institute website (https://singlecell.broadinstitute.org/single_cell/study/SCP1290) and cell type annotation and Uniform manifold approximation and projection (UMAP) coordinates were retrieved and used to generate UMAP plots.

Statistics

Data were expressed as means ± s.e.m. (standard error of the mean). Non-parametric Mann Whitney test (two-tailed) (data sets = 2) and non-parametric Kruskall-Wallis test followed by Dunn's post-hoc test for multiple comparisons (data sets > 2) were used wherever appropriate. Fisher's exact test, with pairwise comparisons and Benjamini–Hochberg correction if needed, was used to assess the overall risks to hindlimb hyperextension and to GTCS, to compare the number of pups exhibiting ictal-like events in extracellular slice recordings, and to verify the lack of sex ratio differences between cohorts (Table S10). The statistical analyses and representation were performed using R version 4.3.1 (R Core Team: The R Project for Statistical Computing, R Foundation for Statistical Computing, Vienna, Austria; https://www.r-project.org/), Rstudio version 2023.06.2 + 561 'Mountain Hydrangea' release (RStudio: Integrated Development Environment for R. Posit Software, PBC, Boston, MA, USA; http://www.posit.co/) and GraphPad Prism version 10.1.1 (GraphPad Software, San Diego, California, USA). Survival analysis was performed using the Kaplan–Meier method, with the survival curves among treatment groups compared using the Log-Rank test. The "survival" and "survminer" packages in R were utilized for survival analysis [43]. The "lsmeans" package was employed for deriving least-squares means and contrasts [44], while the "lme4" package was used for the fitting of mixed models [45]. Scripted R codes used for the analyses are available upon reasonable request. Significance thresholds were set at $p < 0.05$.

Results

Maternal intake of acetylsalicylic acid (aspirin, ASA) during pregnancy reduces the rate of postnatal lethality caused by cytomegalovirus (CMV) infection of the fetal brain

Rat CMV with a green fluorescent protein (GFP) expression cassette [30] was injected in the cerebral ventricles of the embryos from timed pregnant rats at embryonic day 15 (E15), as previously done [20, 21]. Each of the four drugs with immunomodulatory properties was administered to the pregnant dams as from E5-E6 and the treatment was discontinued upon delivery (P0). Our previous studies had indicated a strong statistical correlation between postnatal survival rates on the one hand, and the occurrence of neurologic manifestations on the other hand [21]. Hence, as a first step to rapidly select the most promising drug(s), the impact on postnatal survival was evaluated in first series of treated and untreated CMV-infected pups. In line with previously reported cohorts [21], CMV infection of the fetal brain significantly impacted on postnatal survival ($p < 0.0001$), compared to the non-infected, control group with icv injection of the vehicle (MEM) only (Figure S1A) (Table S1). Amongst the four drugs, only ASA intake during pregnancy led to significant improvement of survival in treated *vs* untreated CMV-infected pups ($p = 0.0203$). Hence, this drug was used in the next experiments.

Altered lipid metabolism and activation of the arachidonic acid-to-prostaglandins synthesis pathway in CMV-infected developing brains

ASA administration during pregnancy improved postnatal survival. In addition, the fluorescent GFP areas corresponding to CMV-infected regions decreased significantly in size in ASA-treated, CMV-infected postnatal brain slices as compared with their untreated counterparts ($p = 0.0155$), suggesting reduced CMV loads in the postnatal brains (Figure S1B) (Table S2). ASA targets Cox-1 and, to a lesser extent, Cox-2 [46, 47]. These enzymes control the production of PGs from arachidonic acid in most cell types. One of the most studied and abundant PG is PGE2, which has been involved in the modulation of viral infections [48]. Owing to the beneficial impact of the cyclooxygenases-targeting drug ASA on postnatal survival in our model, we decided to monitor the production of oxygenated fatty acids including PGs in the CMV-infected brains

using targeted lipidomics. To this aim, oxygenated fatty acids were extracted from CMV-infected and non-infected whole brains at E17 and at P1 and subjected to quantitative analysis by mass spectrometry (Fig. 1) (Figures S2, S3, Table S3). While not yet detectable at E17, PGE2 and its downstream product thromboxane B2 (TxB2) showed significant increases in CMV-infected brains at P1 (PGE2: 1.179 ± 0.128 ng/g of brain tissue; TxB2: 0.885 ± 0.106 ng/g of brain tissue), as compared with uninfected controls (PGE2: 0.551 ± 0.061 ng/g of brain tissue; TxB2: 0.473 ± 0.088 ng/g of brain tissue) (PGE2: $p = 0.0073$; TxB2: $p = 0.0170$). Maternal intake of ASA decreased, albeit not significantly, the PGE2 and TxB2 levels in CMV-infected brains at P1 (PGE2: 0.853 ± 0.176 ng/g of brain tissue; TxB2: 0.59 ± 0.111 ng/g of brain tissue), that is 24h after the treatment had been discontinued (Fig. 1) (Table S3). Besides, at E17 the levels of the hydroxyoctadecadienoic acid (HODE) derivatives of linoleic acid, 9(S) HODE and 13(S) HODE, were significantly decreased ($p = 0.0123$ and $p = 0.0178$, respectively) in the infected brains (9(S) HODE: 1.89 ± 0.665 ng/g of brain tissue; 13(S) HODE: 1.366 ± 0.39 ng/g of brain tissue) compared to non-infected brains (9(S) HODE: 3.128 ± 0.266 ng/g of brain tissue; 13(S) HODE: 1.616 ± 0.22 ng/g of brain tissue). When the ratio of 13- to 9-HODE taken as a readout of immune response to viral infection [49] was calculated, the trend ($p = 0.0662$) for increased ratio seen in the CMV-infected brains at E17 was significantly reverted by ASA ($p < 0.0001$). Notably, at P1 the ratio was not modified in the CMV condition, and was even increased in the CMV + ASA group ($p = 0.0434$). None of the lipoxygenase-dependent metabolites of arachidonic acid, namely 5(S), 8(S), 11(S), 12(S) and 15(S) hydroxyeicosatetraenoic acids (HETE) was dysregulated at E17. At P1, apart from the aforementioned increases in PGE2 and in TxB2, 20(S) HETE, a cytochrome P450 (CYP450)-dependent metabolite of arachidonic acid, was significantly downregulated ($p = 0.0075$) in the CMV-infected brains.

In CMV-infected fetal brains, the increased proportion of microglial cells expressing cyclooxygenase-1 is reverted upon in utero administration of ASA

The efficacy of ASA in our model and the increased production of PGE2 and TxB2 in the CMV-infected developing brains then led us to analyze the expression status of Cox-1 and Cox-2. qRT-PCR experiments detected a significant increase in the expression of *Ptgs1* (Cox-1 gene), but not *Ptgs2* (Cox-2 gene), in RNAs extracted from CMV-infected neonatal brains at P1, as compared with control (MEM-injected) brains (n = 10 each) (*Ptgs1*: $p = 0.0175$; *Ptgs2*: $p = 0.1051$) (Figure S4) (Table S4). Besides, analysis of single cell RNAseq data from the developing (E10 to P4) mouse cerebral cortex [42] at the Broad Institute website revealed prominent expression of Cox-1 and, to a lesser extent, of Cox-2, in microglial cells during brain development (Figure S5). Furthermore, ASA was previously shown to decrease the microglial overexpression of the Cox-1 protein in inflammatory conditions [50]. We thus decided to more selectively monitor the microglial expression of Cox-1 and Cox-2 in our model. Immunohistochemistry experiments revealed a significant increase in the density of microglial cells ($Iba1^+$) in CMV-infected fetal brains compared to non-infected fetal brains at E17 in the two independent series of Cox1- and Cox2-related experiments ($p = 0.0465$ and $p = 0.0184$, respectively) (Fig. 2) (Table S5). Importantly, CMV-infected fetal brains at E17 displayed significantly increased proportions of microglial cells expressing either of Cox-1 ($Cox\text{-}1^+$: 8.134% ± 0.714) or Cox-2 ($Cox\text{-}2^+$: 8.769% ± 1.388), compared to the non-infected condition ($Cox\text{-}1^+$: 2.628% ± 0.597) ($Cox\text{-}2^+$: 2.049% ± 0.67) (Cox-1: $p < 0.0001$; Cox-2: $p = 0.0038$). While having no effect on the increased density of microglial cells, maternal intake of ASA reverted the increased proportion of $Cox\text{-}1^+$ microglia ($p = 0.0494$) at E17 ($Cox\text{-}1^+$: 4.759% ± 0.654), as compared with untreated, CMV-infected brains. In contrast, ASA had no significant effect on the increased proportion of $Cox\text{-}2^+$ microglia seen at E17 ($Cox\text{-}2^+$: 10.22% ± 1.87) in CMV-infected brains (Fig. 2) (Table S5). The effect of ASA on $Cox\text{-}1^+$ microglia was transient only: at P1, that is 24 h after drug discontinuation, significant and comparable increases

(See figure on next page.)

Fig. 1 Dysregulated fatty acid oxidation pathways and overactivation of the arachidonic acid-to-PG pathway in CMV-infected brains. **A** Oxygenated fatty acids derived from linoleic acid (HODE) and arachidonic acid (HETE, PgE2 and TxB2) analyzed by mass spectrometry in the present study. **B**, **C** Brain content of the different oxygenated fatty acids of interest (derived from linoleic or arachidonic acid). Only data for lipids showing significant dysregulation in CMV-infected brains at E17 (**B**) and at P1 (**C**) are shown (see Figure S3 for all other lipids); a statistical trend obtained with the ratio of 13- to 9-HODE at E17 is also indicated. MEM: non-infected brains (E17: n = 8, 1 litter; P1, n = 9, 3 litters); CMV: untreated, CMV-infected brains (E17: n = 12, 1 litter; P1: n = 8, 2 litters); CMV + ASA: ASA-treated, CMV-infected brains (E17: n = 11, 1 litter; P1: n = 8, 2 litters). ****: $p < 0.0001$; **: $p < 0.01$; *: $p < 0.05$; ns: not significant. Kruskal–Wallis test with Dunn's post-hoc correction

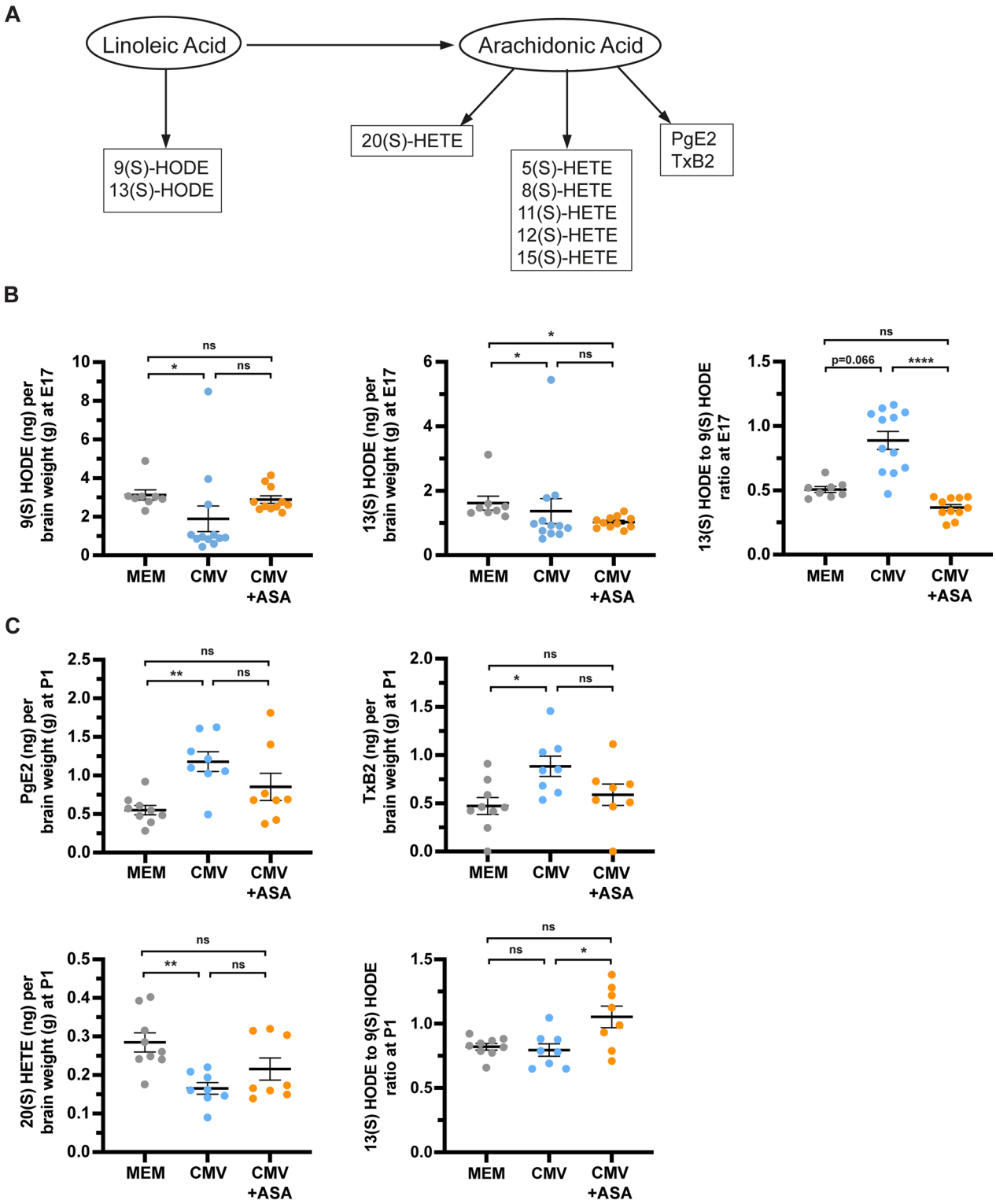

Fig. 1 (See legend on previous page.)

in the proportion of Cox-1$^+$ microglia were detected in both the untreated (22.29% ± 3.026) and the ASA-treated (24.37% ± 2.68) CMV-infected brains ($p = 0.0009$ and $p = 0.0001$, respectively, compared with non-infected brains: 6.085% ± 1.1) (Fig. 3) (Table S5). Similarly, the increased proportion of Cox-2$^+$ microglia detected at P1

in CMV-infected brains (12.35% ± 1.594) as compared with the non-infected brains (5.174% ± 0.65) ($p = 0.007$) was not significantly modified ($p = 0.768$) by ASA intake during pregnancy (9.114% ± 0.95) (Fig. 3) (Table S5), as also observed at E17 (Fig. 2) (Table S5). In summary, CMV infection of the fetal brain led to increased proportions of Cox-1^+ and Cox-2^+ microglia at E17 and at P1. ASA treatment transiently reduced the proportion of Cox-1^+ microglia at E17 but no longer at P1, after ASA had been discontinued, while having no significant effect on the increased proportion of Cox-2^+ microglia at either developmental stage.

ASA administered during pregnancy, but not the Cox-1 knock-out, improves the postnatal phenotypes caused by cytomegalovirus (CMV) infection of the fetal brain

ASA reverted the increase of Cox-1 expression in fetal microglia from CMV-infected brains. It also improved postnatal survival. More comprehensive evaluations of neurologic postnatal phenotypes were performed in larger cohorts on a daily basis during the first postnatal weeks. Two different strategies aimed at targeting the PG pathway and Cox-1 particularly were used: pharmacological targeting with ASA intake during pregnancy as done above, and genetic knock-out of *Ptgs1* for more selective targeting of Cox-1.

The efficacy of ASA administered to the pregnant dam was assessed in CMV-infected pups compared with their CMV-infected counterparts born from untreated dams (Fig. 4) (Table S6). In addition to ASA, NAC administration was also evaluated here as postnatal survival seemed to be slightly improved, albeit not significantly, in the two first NAC-treated cohorts that had been analyzed formerly, and as the respective impacts of NAC and ASA on survival were not significantly different from each other in the former cohorts (Figure S1A) (Table S1). As a matter of fact, the aforementioned beneficial impact of ASA on the postnatal survival rates was confirmed with the additional CMV-infected cohorts analyzed here (ASA-treated *vs* untreated: $p = 0.009$) (Fig. 4A); moreover, NAC also led to significant improvement of survival (NAC-treated *vs* untreated: $p = 0.041$). ASA and NAC also led to: (i) increased body weight gain (ASA-treated *vs* untreated: $p < 0.0001$; NAC-treated *vs* untreated: $p < 0.0001$) (Fig. 4B); (ii) improved sensorimotor development, as assessed by the successes to the righting reflex test (ASA-treated vs untreated: $p < 0.0001$; NAC-treated vs untreated: $p < 0.001$) (Fig. 4C) and to the cliff aversion reflex test (ASA-treated *vs* untreated: $p < 0.0001$; NAC-treated *vs* untreated: $p < 0.001$) (Fig. 4D); and (iii) decreased occurrence of hindlimb hyperextension (ASA-treated *vs* untreated: $p < 0.0001$; NAC-treated *vs* untreated: $p < 0.001$) (Fig. 4E). When only the pups who succeeded to the sensorimotor tests were compared, times required to perform successfully were significantly improved after ASA treatment (righting reflex: $p < 0.0001$; cliff aversion reflex: $p = 0.0294$) while they did not change after NAC treatment (righting reflex: $p = 0.197$; cliff aversion reflex: $p = 0.935$) (Figure S6). Furthermore, ASA, but not NAC, led to a 24 to 48 h delay in the overall occurrence of GTCS triggered by handling (ASA-treated *vs* untreated: $p = 0.0311$; mixed model for repeated measures) (Fig. 4F); however, while GTCS were seen in 10 out of the 41 CMV-infected pups and never in any of the 30 MEM pups ($p = 0.00564$; Fisher's exact test, two-tailed), ASA did not impact on the overall risk to GTCS (ASA-treated *vs* untreated: $p = 0.37$; Fisher's exact test, two-tailed) (Figure S6).

Upon administration to the pregnant dam, ASA performed better than NAC in improving the postnatal phenotypes caused by CMV infection of the fetal brain in utero, as had been previously suggested by their respective effects on postnatal survival in the first cohorts analyzed (Figure S1A). ASA exhibits a higher inhibitory potency against Cox-1 than against Cox-2 [46, 47], and reverted the increased Cox-1 microglial expression in the CMV-infected fetal brains. Altogether, these data raised the possibility that Cox-1 participates in CMV-related

(See figure on next page.)

Fig. 2 Maternal intake of aspirin reverts the increased microglial expression of Cox-1 in CMV-infected fetal brains. Cox-1 and Cox-2 microglial expressions were quantified in brains from non-infected (MEM) cohort and in brains from untreated (CMV) and ASA-treated (CMV + ASA) infected cohorts, all from two litters each, using immunohistochemistry. **A** Cells were quantified in a region of interest (ROI; red square) located in the dorsolateral corner of the lateral ventricle, in brain sections selected at the same anatomical level (plate 30–57; see http://larrywswanson.com/?page_id=936) [40]. **B** Representative confocal images (coronal sections) of embryonic brains at E17 after immunohistochemical stainings for Iba1$^+$ cells (microglia; magenta) and for Cox-1$^+$ (cyan, left panels) and Cox-2$^+$ (cyan, right panels) cells in the three experimental conditions. Scale bars apply to all corresponding images and insets (dashed squares). Left and right insets are labeled with one and two stars, respectively. White arrowheads point to co-labeled Iba1$^+$, Cox-1$^+$ or Iba1$^+$, Cox-2$^+$ cells. Orange arrows point to Iba1$^+$, Cox1$^-$ or Iba1$^+$, Cox2$^-$ cells. (C) (top) Densities of microglia (Iba1$^+$ cells) were calculated as the total number of Iba1 + cells per µm^2 of brain section. (bottom) The proportions of microglia (Iba1$^+$) expressing either of Cox-1 or Cox-2 were quantified by calculating the ratio of Iba1$^+$, Cox-1$^+$, or Iba1$^+$, Cox-2$^+$ cells to the total number of Iba1$^+$ cells. Cox-1 series: MEM: n = 12; CMV: n = 11; CMV + ASA: n = 11. Cox-2 series: MEM: n = 11; CMV: n = 11; CMV + ASA: n = 12. ****: $p < 0.0001$; ***: $p < 0.001$; **: $p < 0.01$; *: $p < 0.05$; ns: not significant. Kruskal–Wallis test with Dunn's post-hoc correction

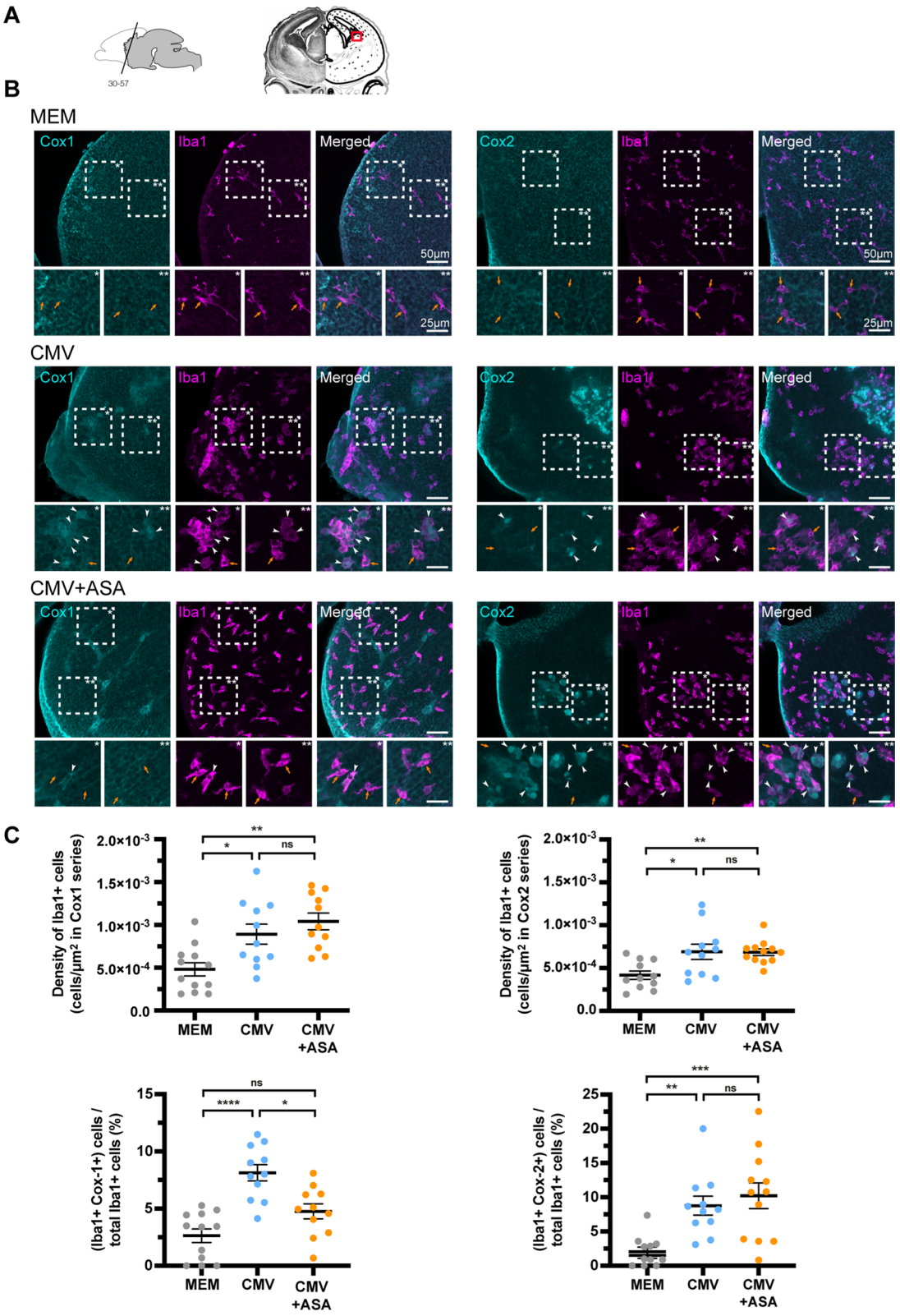

Fig. 2 (See legend on previous page.)

neurodevelopmental pathogenesis. Cox-1 KO embryonic brains were thus infected with CMV to see if the constitutional lack of Cox-1 would recapitulate the effects of ASA against CMV-associated pathogenesis. However, none of the beneficial effects of ASA on the postnatal phenotypes was seen in the CMV-infected Cox-1 KO pups in vivo as compared with their wild-type counterparts (Fig. 5) (Table S7).

Both ASA treatment in utero and the Cox-1 knock-out prevent against spontaneous epileptiform activity in neocortical slices from CMV-infected pups

Maternal ASA intake during pregnancy had an undisputable beneficial impact on the severe, postnatal neurologic phenotypes caused by CMV infection of the fetal brain. However, the improvement of GTCS looked more subtle, as ASA only led to a delay in the occurrence of GTCS in treated *versus* untreated pups. To further evaluate the effect of ASA treatment in utero on neuronal network activity in the CMV-infected brains, extracellular electrophysiological recordings were then performed ex vivo in layer IV of somatosensory cortices taken from pups aged 14–16 days (P14-P16). Spontaneous ictal-like events were detected in brain slices from each of the five CMV-infected pups analyzed (Fig. 6A, B), while, as expected, no slice from five control (MEM) pups showed such events ($p=0.0228$) (Fig. 6C). The averaged frequency distribution of spikes within the ictal-like events revealed a bimodal distribution with two peaks occurring at around 13 Hz and 23 Hz, respectively (Fig. 6B) (Table S8). Maternal ASA intake during pregnancy led to a significant recovery, as only one out of six ASA-treated, CMV-infected pups showed a spontaneous ictal-like event ($p=0.0228$) (Fig. 6C). We then analyzed the spontaneous unitary spikes (Fig. 6D), which were categorized as interictal-like events, focusing on a 5-min representative time interval where the previously-identified ictal-like events were absent. The averaged frequency distribution of interictal spikes within the selected time interval revealed a single peak at approximately 3 Hz (Fig. 6E) (Table S8). A significant increase in the mean frequency of spontaneous interictal-like events was observed in slices from untreated, CMV-infected pups compared to slices from control (MEM) pups ($p=0.032$); this increase was significantly counteracted in slices obtained from ASA-treated, CMV-infected pups ($p=0.0002$) (Fig. 6F) (Table S8).

Consistently, spontaneous ictal-like events were never detected in slice recordings from seven CMV-infected, Cox-1 KO pups, while most (six out of eight) CMV-infected, wild-type pups showed such ictal-like events ($p=0.007$) (Fig. 7A–C). The frequency distribution of spikes within these ictal-like events displayed a unimodal distribution with a peak at approximately 13 Hz (Fig. 7B) (Table S9). Analysis of the interictal-like events (Fig. 7D) revealed a mean frequency distribution of spikes peaking at 3 Hz (Fig. 7E) (Table S9). As with ASA intake in utero, a significant and dramatic reduction in the occurrence of interictal-like events was seen in slices from CMV-infected Cox-1 KO pups compared to their CMV-infected WT counterparts ($p<0.0001$) (Fig. 7F) (Table S9).

In summary, whereas no improvement of the postnatal epileptic outcome of CMV infection was obtained in vivo in Cox-1 KO pups, an undisputable beneficial effect of Cox-1 KO on the epileptiform events was obtained ex vivo as with ASA in neocortices from CMV-infected pups.

Discussion

The involvement of early altered cellular and molecular immune processes in the neuropathogenesis of congenital CMV infection has been increasingly questioned in the recent years. In a model of CMV infection of the developing rat brain in utero [20, 21], we now provide evidence for overproduction of PGE2—one main product of the PG synthesis pathway—in the developing brain

(See figure on next page.)

Fig. 3 Maternal aspirin intake does not rescue Cox-1 and Cox-2 microglial overexpressions in CMV-infected neonatal brains. Cox-1 and Cox-2 microglial expressions were quantified in brains from non-infected (MEM) cohort (three litters) and in brains from untreated (CMV) (four litters) and ASA-treated (CMV + ASA) (three litters) infected cohorts, using immunohistochemistry. **A** Cells were quantified in a region of interest (ROI; red square) located in the dorsolateral corner of the lateral ventricle, in brain sections selected at the same anatomical level (bregma + 0.8 mm; see https://www.inmed.fr/en/en-atlas-stereotaxique-du-cerveau-de-rat-au-cours-du-developpement-postnatal) [41]. **B** Representative confocal images (coronal sections) of embryonic brains at P1 after immunohistochemical stainings for $Iba1^+$ cells (microglia; magenta) and for $Cox\text{-}1^+$ (cyan, left panels) and $Cox\text{-}2^+$ (cyan, right panels) cells in the three experimental conditions. Scale bars apply to all corresponding images and insets (dashed squares). Left and right insets are labeled with one and two stars, respectively. White arrowheads point to co-labeled $Iba1^+$, $Cox\text{-}1^+$ or $Iba1^+$, $Cox\text{-}2^+$ cells. Orange arrows point to $Iba1^+$, $Cox1^-$ or $Iba1^+$, $Cox2^-$ cells. **C** (top) Densities of microglia ($Iba1^+$ cells) were calculated as the total number of Iba1 + cells per μm^2 of brain section. (bottom) The proportions of microglia ($Iba1^+$) expressing either of Cox-1 or Cox-2 were quantified by calculating the ratio of $Iba1^+$, $Cox\text{-}1^+$, or $Iba1^+$, $Cox\text{-}2^+$ cells to the total number of $Iba1^+$ cells. Cox-1 series: MEM: n = 11; CMV: n = 12; CMV + ASA: n = 13. Cox-2 series: MEM: n = 12; CMV: n = 12; CMV + ASA: n = 13. ***: $p<0.001$; *: $p<0.05$; ns: not significant. Kruskal–Wallis test with Dunn's post-hoc correction

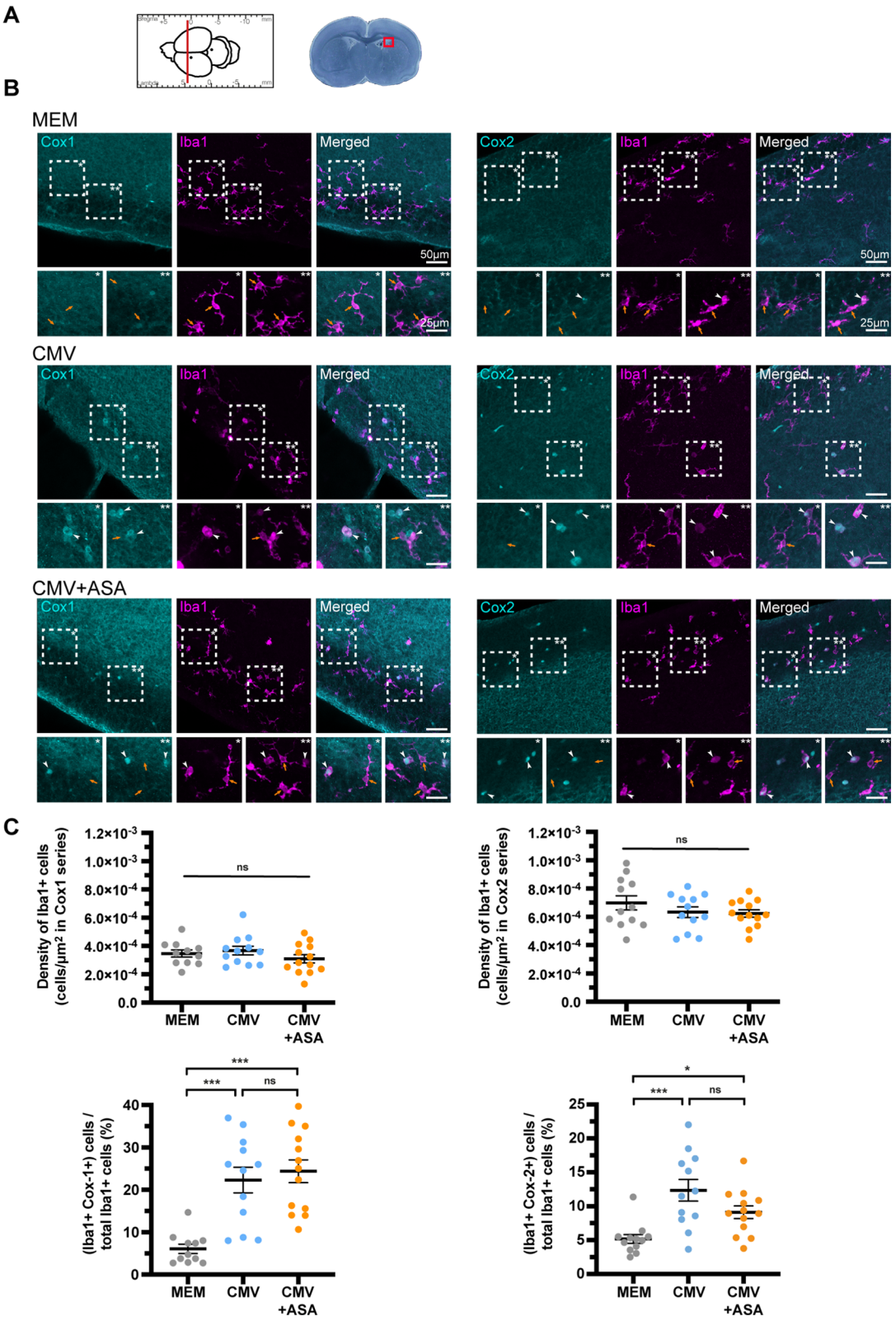

Fig. 3 (See legend on previous page.)

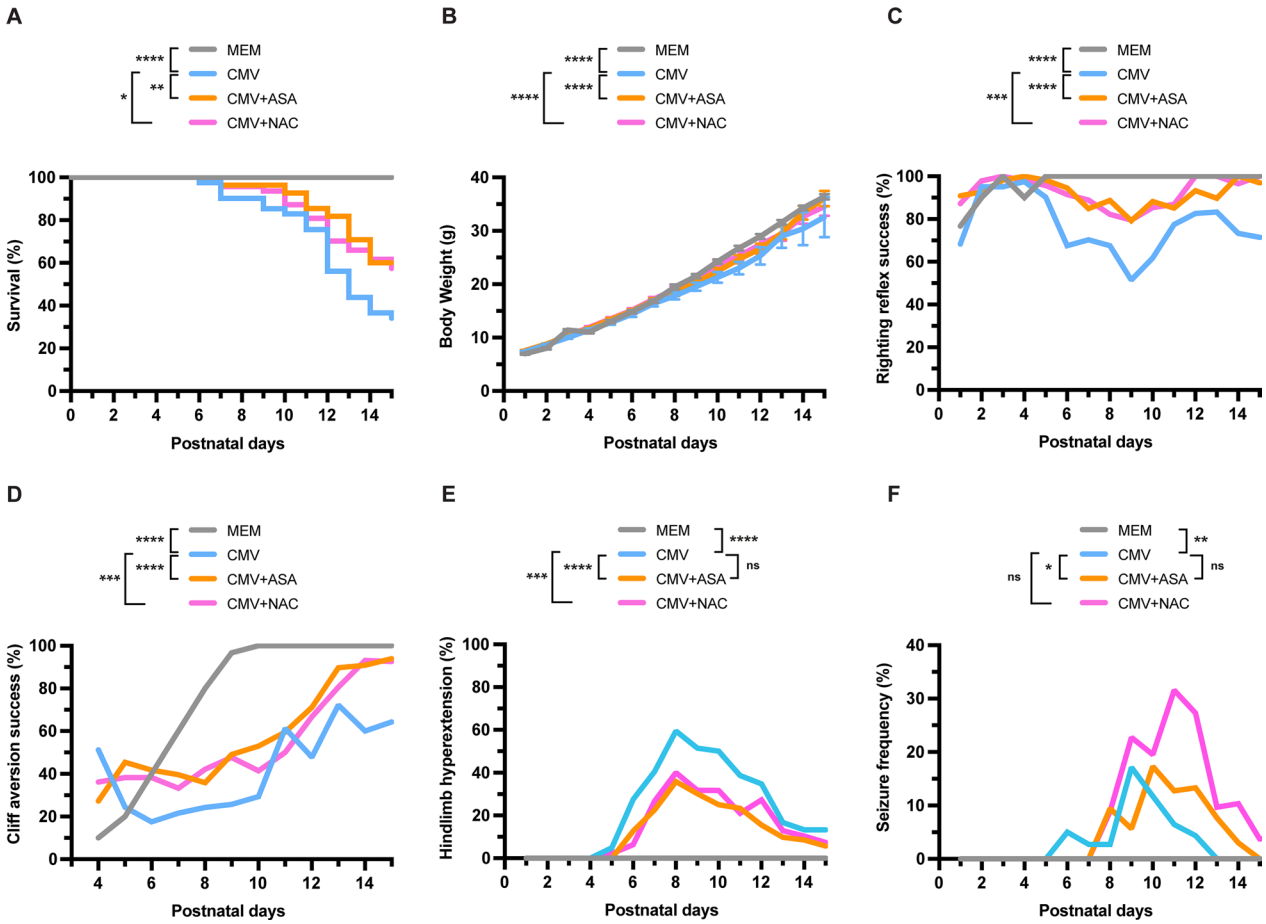

Fig. 4 Maternal aspirin improves the in vivo postnatal phenotypes after CMV infection of the fetal brain. Postnatal phenotyping was done as reported previously [21] on a daily basis during the two first postnatal weeks by comparing cohorts of rat pups previously submitted to icv injections of MEM (vehicle) or of CMV at E15. CMV cohorts were untreated or treated with either of acetylsalicylic acid (ASA) or N-acetyl-L-cysteine (NAC) provided to the dam in drinking water ad libitum from E5-6 until delivery. MEM: non-infected cohort (n = 30 from three litters); CMV: CMV-infected, untreated cohort (n = 41 from five litters); CMV + ASA: CMV-infected, ASA-treated cohort (n = 55 from six litters); CMV + NAC: CMV-infected, NAC-treated cohort (n = 47 from six litters). Sex ratio did not differ significantly between the four conditions at birth ($p = 0.7497$, Fisher's exact test). As reported [21], CMV infection worsened the postnatal phenotypes, compared to the MEM cohort. Both the CMV + ASA and the CMV + NAC cohorts displayed significant improvements in: **A** survival; **B** body weight gain; **C** success to the righting reflex test; **D** success to the cliff aversion test; **E** occurrence of hindlimb hyperextension. **F** ASA, but not NAC, led to a significant delay in the occurrence of GTCS. **E**–**F** In addition to the mixed model (left statistics), Fisher's exact test (right statistics) was used to assess the overall risks to hindlimb hyperextension (**E**) and to GTCS (**F**) in the MEM, CMV-infected and ASA-treated cohorts (see also Figure S6B). Note that due to the previously reported relationship between survival on the one hand and the neurologic phenotypes on the other hand [21], a misleading effect of apparent improvement with time could be perceived. ****: $p < 0.0001$,***: $p < 0.001$; **: $p < 0.01$; *: $p < 0.05$; ns: not significant. Kaplan–Meier method followed by Log-Rank test (**A**); mixed model for repeated measures (**B**–**F**); Fisher's exact test, two-tailed, with pairwise comparisons and Benjamini–Hochberg correction (**E**, **F**)

following CMV infection, and we show that expressions of Cox-1 and of Cox-2, the two key enzymes of the PG pathway, are increased in microglia in such a context. In this model, we also show that maternal intake during pregnancy of ASA, a drug known to inhibit the PG pathway, reverted the Cox-1 overexpression seen in fetal microglia, improved postnatal survival and the severity of the postnatal neurologic phenotypes, and prevented against the epileptiform events recorded in neocortical slices from CMV-infected pups. While Cox-1 KO had no such a beneficial effect on CMV-infected pups in vivo, the CMV-related epileptiform events were successfully prevented as with ASA in Cox-1 KO ex vivo.

CMV, microglia, ASA, and cyclooxygenases

Viral infections may impact on brain development via impaired microglia functioning [51]. Our previous data had indicated that fetal microglia was pivotal to the neuropathogenesis associated with CMV infection of the fetal brain [21], which is consistent with the

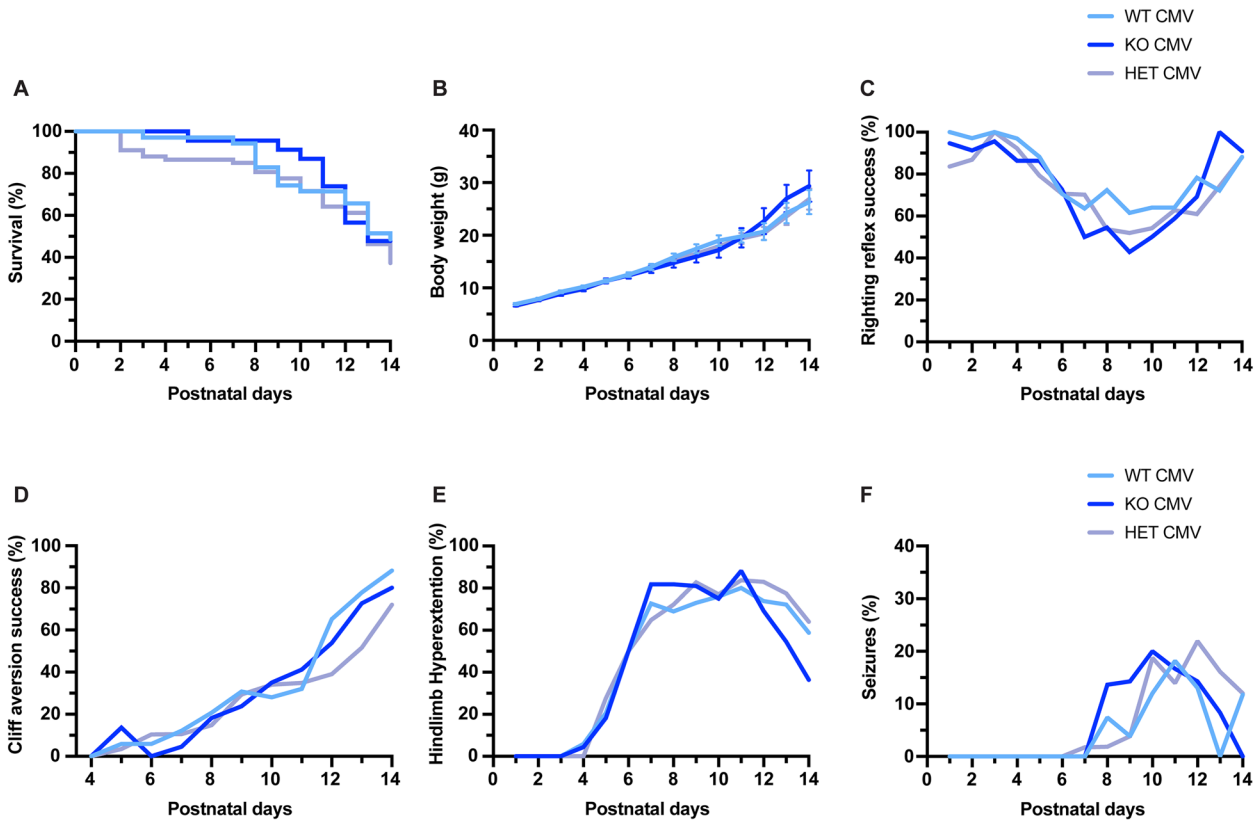

Fig. 5 Cox-1 knock-out does not improve the in vivo postnatal phenotypes after CMV infection of the fetal brain. Postnatal phenotyping was done as reported previously [21] on a daily basis during the two first postnatal weeks in 17 litters with Cox-1$^{+/+}$ (wild-type, WT; n = 35), Cox-1$^{\pm}$ (heterozygotes, HET; n = 67) and Cox-1$^{-/-}$ (homozygotes knock-out, KO; n = 23) rat pups previously submitted to icv injections of CMV at E15. Sex ratio did not differ significantly between the three conditions at birth (p = 0.2489, Fisher's exact test). No significant improvement was observed in Cox-1$^{-/-}$ and in Cox-1$^{\pm}$ pups compared to Cox-1 WT pups for **A** survival **B** body weight gain **C** success to the righting reflex test **D** success to the cliff aversion test **E** occurrence of hindlimb hyperextension **F** generalized tonic–clonic epileptic seizures. Of note, success to the righting reflex test even worsened significantly (p = 0.0223) in Cox-1$^{-/-}$ rats compared to Cox-1 WT. Kaplan–Meier method followed by Log-Rank test (**A**); mixed model for repeated measures (**B–F**)

crucial role of microglia not only in immune defense against pathogens, but also in various developmental processes such as neurogenesis, synaptogenesis, synaptic pruning, and connectivity [52, 53]. We had shown that drug-based transient rescue of altered fetal microglia during pregnancy was sufficient to prevent against the neurologic phenotypes postnatally [21]. The present data are in line with these findings: the effect of maternal intake of ASA, reducing Cox-1 expression in fetal microglia at E17 but not at P1, was associated with a beneficial impact on the postnatal phenotypes in vivo, and on the epileptiform events recorded in the neocortex of rat pups ex vivo. This is consistent with previous reports showing that ASA reduced the inflammation-induced overexpression of Cox-1 protein in microglial cells [50], and that Cox-1 inhibitors could revert the increased expression of Cox-1 in microglial cells stimulated with lipopolysaccharide [54].

ASA acts by acetylating Cox-1 at serine 529 and Cox-2 at serine 516, and is rapidly deacetylated into salicylic acid. Both ASA and salicylic acid have relatively short half-lives (20 min and 2–4.5 h, respectively) [55]. This could explain the lack of any apparent impact of ASA on microglial Cox-1 expression observed in the neonatal brains at P1, i.e., 24 h after maternal treatment discontinuation. The mechanisms of action of salicylic acid remain debated. Salicylic acid may have no efficient effect on Cox activities but would rather decrease PG synthesis by inhibiting Cox production. As a matter of fact, ASA was previously shown to decrease the inflammation-induced overexpression of the Cox-1 protein in microglia [50] and of the Cox-2 gene (*Ptgs2*) in macrophages [37].

While a classical view has long considered that inducible Cox-2 expression was prominently involved upon inflammatory challenge, a critical proinflammatory

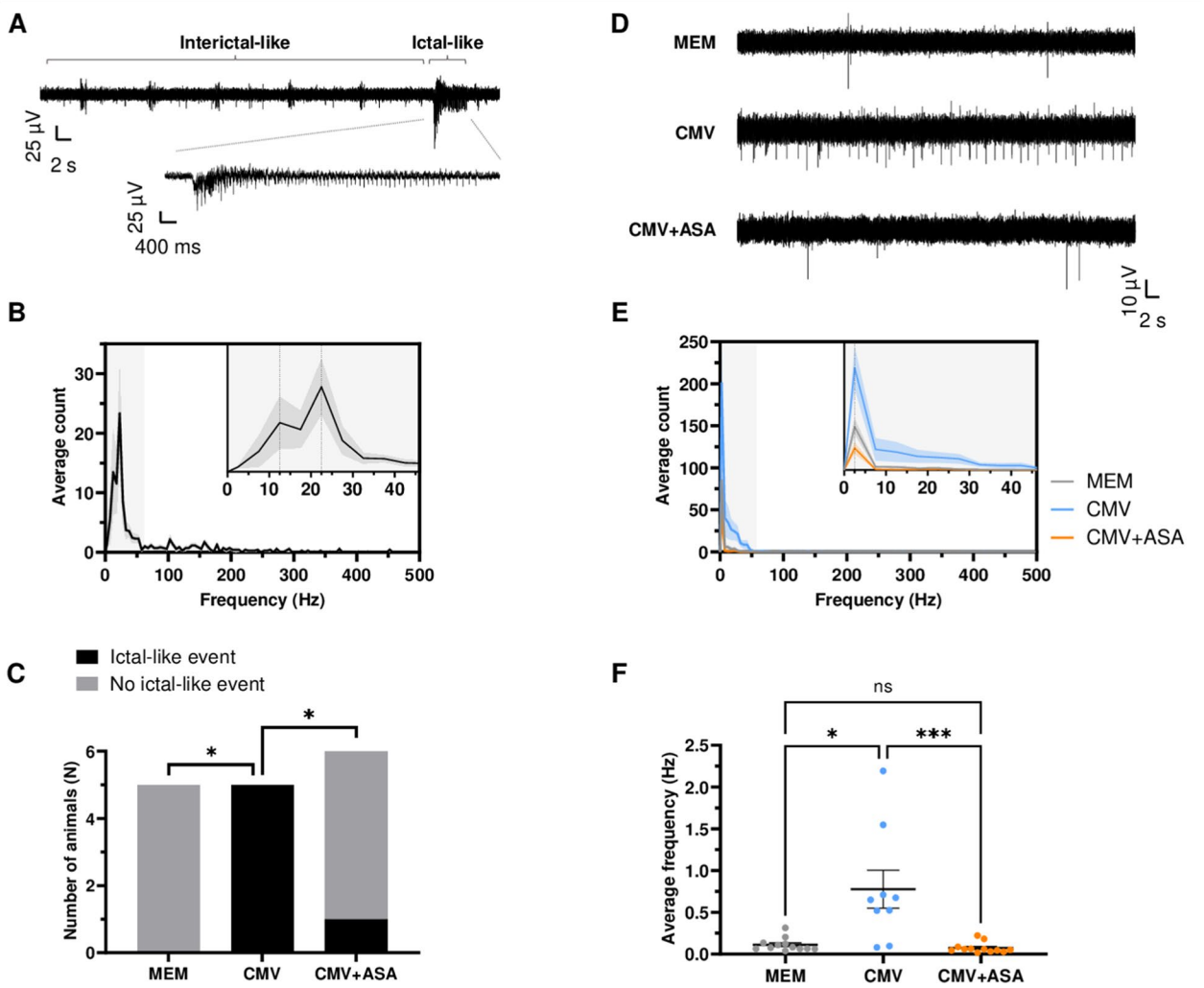

Fig. 6 Maternal aspirin intake prevents against ictal- and interictal-like events in CMV-infected postnatal brains ex vivo. **A** Representative local field potential (LFP) trace of spontaneous events recorded at P15 within the neocortical layer IV in brain slices from CMV-infected rat pups (top). The ictal-like event is shown at an expanded timescale (bottom). **B** Mean frequency distribution of spikes for ictal-like events (n = 7 events in brain slices from five CMV-infected pups (two litters)). Bin size was set at 5 Hz. Average count values corresponding to the middles of each bin are connected with a solid line. A zoom-in of the initial part (0–45 Hz) of the frequency distribution is shown on the right corner. **C** Proportion of pups exhibiting ictal-like events in different conditions: control (MEM); untreated, CMV-infected (CMV); and ASA-treated, CMV-infected (CMV + ASA). *: $p < 0.05$. Fisher's exact test, two-tailed, with pairwise comparisons and Benjamini–Hochberg correction. **D** Representative LFP traces of spontaneous interictal-like events recorded in brain slices from control (MEM, top trace), untreated CMV-infected (CMV, middle trace), and ASA-treated CMV-infected (CMV + ASA, bottom trace) pups. **E** Mean frequency distribution of spikes for interictal-like events. Control (MEM, grey trace, n = 12 slices from five pups (two litters)); untreated CMV-infected (CMV, blue trace, n = 9 slices from five pups (two litters)); ASA-treated CMV-infected (CMV + ASA, orange trace, n = 12 slices from six pups (three litters)). A zoom-in of the initial part (0–45 Hz) of the frequency distribution is shown on the right corner. **F** Summary data for averaged spike frequencies for interictal-like events in control (MEM, left, n = 12 slices from five pups (two litters)), untreated CMV-infected (CMV, middle, n = 9 slices from five pups (two litters)) and ASA-treated CMV-infected (CMV + ASA, right, n = 12 slices from six pups (three litters)) conditions. ***: $p < 0.001$; *: $p < 0.05$; ns: not significant. Kruskal–Wallis test with Dunn's multiple comparisons test

function has also been attributed to Cox-1 [56]. Cox-1 and Cox-2 show different expression profiles in the brain and might exert various and sometimes opposite roles in neuroinflammation [56]. There is more prominent expression of *Ptgs1* than *Ptgs2* in mouse microglia, according to RNAseq databases (https://www.brainrnaseq.org/; [57] (http://neuroexpresso.org/,[58]), and notably during brain development, as shown by our in silico search at the Broad Institute website (https://singlecell.broadinstitute.org/single_cell/study/SCP1290, [42].

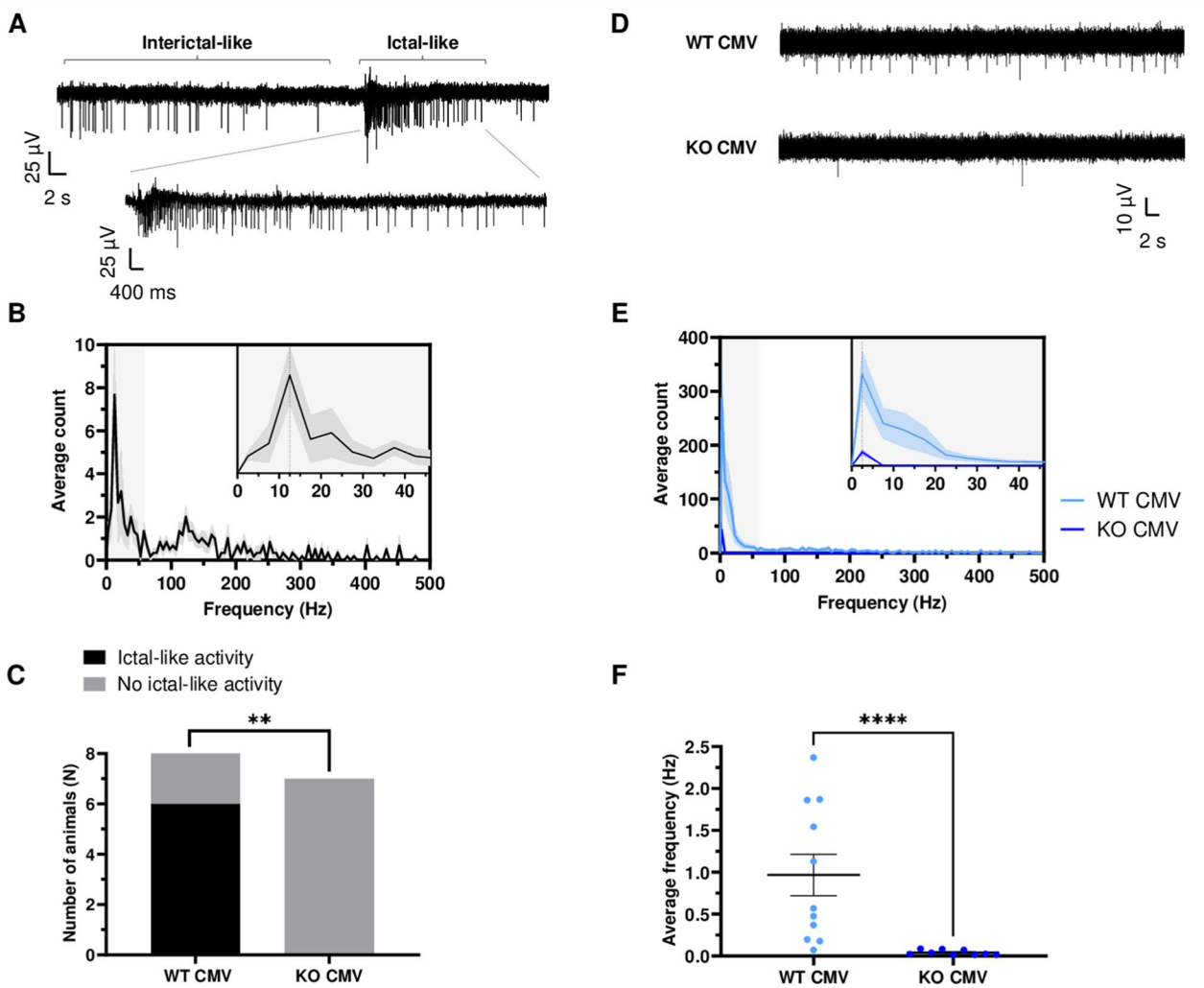

Fig. 7 Cox-1 knock-out prevents against ictal- and interictal-like events in CMV-infected postnatal brains ex vivo. **A** Representative LFP trace of spontaneous events recorded at P15 within the neocortical layer IV in brain slices from wild-type (WT) rat pups infected with CMV (top). The ictal-like event is shown at an expanded timescale (bottom). **B** Mean frequency distribution of spikes for ictal-like events (n = 6 events in brain slices from eight CMV-infected WT pups (four litters)). Bin size was set at 5 Hz. Average count values corresponding to the middles of each bin are connected with a solid line. A zoom-in of the initial part (0–45 Hz) of the frequency distribution is shown on the right corner. **C** Proportion of pups exhibiting ictal-like events in different groups: CMV-infected, WT pups (WT CMV); CMV-infected, Cox-1 KO pups (KO CMV). **: $p < 0.01$. Fisher's exact test, two-tailed. **D** Representative LFP traces of spontaneous interictal-like events recorded in brain slices from CMV-infected WT (top trace) and CMV-infected Cox-1 KO (bottom trace) pups. **E** Mean frequency distribution of spikes for interictal-like events. CMV-infected WT (WT CMV): light blue trace, n = 12 slices from six pups; CMV-infected Cox-1 KO (KO CMV): dark blue trace, n = 9 slices from six pups; all pups from the same four litters. A zoom-in of the initial part (0–45 Hz) of the frequency distribution is shown on the right corner. **F** Summary data for averaged spike frequencies for interictal-like events in CMV-infected WT (WT CMV) pups (right, n = 12 slices from six pups) and from CMV-infected Cox-1 KO (KO CMV) pups (left, n = 9 slices from six pups); all pups from the same four litters. ****: $p < 0.0001$. Mann Whitney test, two-tailed

In our model, ASA intake corrected Cox-1 expression in fetal microglia, while leaving Cox-2 microglial expression unchanged. Interestingly, it was previously shown that rat Cox-1 microglial expression was stimulated under neuroinflammatory challenge [59], and that increased microglial expression of Cox-1, but not Cox-2, was associated with acute cognitive deficits induced by systemic inflammation [60]. Furthermore, a *Ptgs1* (the Cox-1 gene) high-expression allele has been genetically associated with higher risk to cerebral palsy [61], which is one classical and severe outcome of congenital CMV infections. Also, *Ptgs1*, but not *Ptgs2*, is upregulated in brains from HIV-demented *versus* non-demented patients, which likely and selectively sustains the elevated levels of PGE2 found in the cerebrospinal fluids of such HIV-demented patients [62]. It was also shown that

Cox-1 KO mice exhibited attenuated microglia activation in response to brain inflammatory stimuli [27], and that inhibition of Cox-1, but not Cox-2, decreased microglial PGE2 production induced by phagocytosis [63]. Importantly also, the critical involvement of microglial PG synthesis in inflammation-induced negative affect was dependent on Cox-1 [64].

Obviously, the classical limitations of drug-based assays including possible off-target effects should be considered here. Besides microglia, non-microglial cells including other brain phagocytes such as border-associated macrophages, or neuronal cells, would also be targeted by ASA. Also, in line with previous findings [65], ASA intake during pregnancy might even have modified the maternal gut microbiota, which in turn was shown to influence microglia in the offspring [66].

CMV, ASA, and the PG pathway

The possible role of the PG pathway in the neuropathogenesis of congenital CMV infection had not been questioned in vivo yet. PG are lipid molecules produced by the action of cyclooxygenases and PG synthases. PGE2, one of the most studied PG, is an important mediator of inflammation that can be activated in the context of viral infections [48]. Although the impact of CMV infection and of ASA treatment on the production of PGE2 and TxB2 could not be assessed at E17, as they were not detectable by mass spectrometry at that stage, increased amounts of PGE2 were detected in postnatal P1, CMV-infected brain. The increased amounts of PGE2 and the increased proportions of microglial cells expressing Cox-1 or Cox-2 detected here in the CMV-infected brains, as well as the beneficial effects of ASA, are consistent with the known and central role of the PG pathway in neuroinflammation, in microglia homeostasis, and in viral infections [28, 48, 56]. Interestingly, antioxidant agent NAC that also had a favorable impact on the postnatal phenotypes in the present model, was previously shown to decrease PG production [67]. Another product of the PG pathway, namely 15-deoxy-PGJ2, exerts anti-inflammatory effects in part via the peroxisome proliferator-activated receptor γ (PPAR-γ), which has been involved in the neuropathogenesis of congenital CMV infection [68, 69]. Furthermore, the 9- and 13-HODE derivatives of linoleic acid, with 9-HODE being considered pro-inflammatory and 13-HODE anti-inflammatory, are agonists of PPAR-γ [70], and they showed decreased levels here in the CMV-infected brains. Importantly, the ratio of 13- to 9-HODE, which has previously been identified by lipidomic profiling as a putative biomarker for immune response during active viral infection [49], was transiently increased in the CMV-infected fetal brains and this was reverted by ASA, suggesting an anti-inflammatory effect of maternal ASA treatment.

Cox-1-dependent and Cox-1-independent mechanisms for neuropathogenesis and ASA

The data obtained ex vivo in the CMV-infected, Cox-1 KO rats unambiguously demonstrated a beneficial effect of Cox-1 inactivation on the activity of the neuronal networks, at least in layer 4 of the somatosensory cortex, indicating a participation of the PG pathway, and of Cox-1 particularly, in the cerebral alterations caused by congenital CMV infection. However, this was not sufficient to improve the neurologic phenotypes in vivo. In contrast, the beneficial impact of ASA expanded to the phenotypes in vivo. Several non-exclusive reasons could explain this important discrepancy.

First, ASA likely acted via both Cox-1-dependent and Cox-1-independent mechanisms. Notably, while microglial Cox-2 overexpression was not improved by ASA, an additive beneficial effect of ASA via decreased Cox-2 activity and/or production in neurons and other non-microglial cells might be needed to reach successful rescue in vivo. ASA is a pleiotropic drug with multiple and complex effects. Beyond the classical role of ASA and salicylic acid in the inhibition of PG production, both compounds were also shown to act via Cox-independent mechanisms, e.g. via the nuclear factor kappa B (NF-kB) pathway [71, 72], the expression of the interleukin-4 gene [73], or by influencing apoptosis [74]. ASA treatment might have influenced key cellular processes that are disturbed in CMV-infected cells or that have been associated with inflammation, such as cellular senescence [75], the mTOR pathway [76], or PANoptosis [77]—including pyroptosis [78]. Furthermore, ASA was shown to impact on hippocampal plasticity by directly binding to PPAR-α [79]. In a similar vein, it was shown that acetaminophen, a main Cox-2 inhibitor, acted against microglia activation by both Cox-dependent and Cox-independent mechanisms in a mouse model of Down syndrome [80]. Second, compensation might be operating in the context of Cox-1 KO, but not under ASA leading to partial-only inhibition of Cox-1. Indeed, compensatory mechanisms are usually induced against KO but not after gene or protein knockdown [81, 82]. As a related example, it was reported that Cox-1 compensated as the alternative source for PG synthesis in Cox-2 deficient mice [83]. However, the lack of any rescue also seen here in the heterozygous Cox-$1^{+/-}$ pups in vivo would argue against this explanation. Third, the different genetic backgrounds of the naive, Wistar rats used in ASA-based experiments and of the Cox-1 KO, Sprague–Dawley cohorts, might account for differences in Cox-1-dependent responses to CMV infection.

Despite these limitations, Cox-1 inactivation impacted on neurodevelopmental processes in the context of CMV infection, as the KO, despite not having any apparent effect in vivo, rescued the spontaneous epileptiform activities ex vivo. Hence, Cox-1 participated in the detrimental effects that CMV infection of the developing brain and its accompanying brain immune alterations exerted on the activity of the neocortical neuronal networks, as revealed by electrophysiological recordings in both ASA-treated Wistar pups and Cox-1 KO Sprague–Dawley pups. Future studies should help in understanding the likely complicated contribution of the PG pathway to the neuropathogenesis of congenital brain infections. Whether the anomalies triggered by CMV infection of the developing brain, such as the increased microglial Cox-1 and Cox-2 expressions, the disturbed lipid metabolism, or the epileptiform activities, would last longer, and whether longer-term neurologic phenotypes (e.g. altered social interactions) would be seen in older rats—and then, whether such abnormalities would be counteracted by the antenatal treatment with ASA—represent other interesting questions that remain to be addressed. Also, what sustains the improved survival seen with ASA remains undetermined. We had previously found a strong statistical correlation between postnatal lethality and the occurrence of epileptic seizures [21]. Hence, SUDEP (sudden unexpected death in epilepsy) might be postulated, at least in a subset of the pups. In the present study, ASA significantly delayed the occurrence of seizures in the pups, and might also have reduced the risk to SUDEP in the still-epileptic pups, hence contributing to the observed decreased lethality. In addition, ASA might have improved survival by ameliorating the altered sensorimotor skills and hindlimb impairment seen in CMV-infected pups, hence possibly improving feeding—as suggested by increased body weight gain.

Translational perspectives

Our previous [21] and present data provide promising avenues for designing strategies of fetal therapy in human congenital CMV infections. Particularly, the data obtained here represent an in vivo proof-of-principle for the possible use of ASA during pregnancy against the detrimental consequences of congenital CMV infections. Obviously, adapting several aspects of the present study to a possible use in the human condition, such as the doses of ASA, and whether a more time restricted administration of aspirin during pregnancy would also be successful, and whether a critical time window for such an in utero intervention could be defined, notably after CMV infection of the brain, are all important translational issues that should be addressed in future studies. However, it is worth being mentioned that low dose ASA is already one out the few eight approved and proven antenatal interventions aimed at preventing vulnerable birth or at improving outcomes [84], and was shown to improve the future neurobehavioral abilities of very preterm newborns [85].

Conclusion

Maternal administration of ASA during pregnancy improved CMV-related neurodevelopmental abnormalities in the offspring after infection of the rat fetal brain, likely through Cox-1 related and Cox-1 unrelated modes of action. These data represent a first proof-of-principle in vivo for the antenatal use of ASA against the detrimental outcomes of congenital CMV infections.

Supplementary Information

The online version contains supplementary material available at https://doi.org/10.1186/s12974-024-03276-4.

Supplementary Material 1.

Supplementary Material 2.

Acknowledgements

We thank Elodie Bouilloc, Philippe Moudery and Séverine Corby at the INMED (Institut de Neurobiologie de la Méditerranée) animal core facilities, Francesca Bader and Aurélie Montheil at PBMC (Plate-Forme de Biologie Moléculaire et Cellulaire) platform at INMED, Hélène Choubley at DiviOmics platform (Dijon, France), and Dan Streblow at Oregon University (Portland, USA) for providing the GFP-expressing rat CMV strain.

Author contributions

S.T. performed phenotypic evaluations on Cox-1 KO rats, did the electrophysiological experiments and a part of the immunohistochemistry experiments, participated in drug-based phenotypic evaluations on Wistar rats and in lipidomics experiments, performed the related data and statistical analyses, and wrote the manuscript. C.C.-Q. performed drug-based phenotypic evaluations on Wistar rats and participated in the related data analyses. E.B. performed the in utero embryonic infections. L.P. participated in electrophysiological recordings. E.P.-P. performed qRT-PCR experiments and analyses. S.V. did a part of the immunohistochemistry experiments, image acquisition and cell counting analyses. S.S. performed and supervised statistical analyses. L.S. analyzed RNAseq datasets. T.S. performed production and purification of rat CMV. H.L. and C.C. participated in study design and strategy. J.-P.P.B. analyzed and supervised the lipidomics experiments. N.B. supervised electrophysiological recordings and analyses. P.S. supervised data analyses, co-directed study design and overall strategy, participated in lipidomics experiments, and wrote the manuscript. S.B. designed of and participated in drug-based phenotypic evaluations on Wistar and on Cox-1 KO rats as well as in immunohistochemistry experiments, participated in lipidomics experiments, and supervised data analyses, co-directed study design and overall strategy, and wrote the manuscript. All authors read and approved the final manuscript.

Funding

Sarah Tarhini is a recipient of an Aix-Marseille University/A*MIDEX/CMA CGM PhD fellowship and is a member of the Neuroschool PhD program. Carla Crespo-Quiles has been a recipient of a joint INSERM (Institut National de la Santé et de la Recherche Médicale)/Aix-Marseille University/A*MIDEX PhD fellowship. Louison Pineau has been a recipient of a Ministry of Research Aix-Marseille University Doctoral School (ED62) PhD fellowship. Saswati Saha has been a recipient of a CENTURI (Turing Centre for Living Systems)

postdoctoral fellowship. This work was supported by INSERM (Institut National de la Santé et de la Recherche Médicale), by the French 'Investissements d'Avenir' programme with reference ANR-11-LABX-0021 (LipSTIC Labex), by an Excellence Initiative of Aix–Marseille University/A*MIDEX grant (CALIN—R24002AA) of the French 'Investissements d'Avenir' programme, by the French government under the "France 2030" program via A*Midex (Initiative d'Excellence d'Aix-Marseille Université, AMX-19-IET-004) and ANR funding (ANR-17-EURE-0029) to NeuroMarseille/Neuroschool, by the NRJ/Institut de France Foundation, and by FRC (Fédération de Recherche sur le Cerveau).

Availability of data and materials

All data generated or analysed during this study are included in this published article and its supplementary information file (Tables S1-S10).

Declarations

Ethics approval

Animal experimentations were performed in accordance with the French legislation and in compliance with the European Communities Council Directives (2010/63/UE). This study was approved under the French department of agriculture and the local veterinary authorities by the Animal Experimentation Ethics Committee (Comité d'Ethique en Expérimentation Animale) n°014 under licences n°01010.02, n°7256–2016100715494790 v3 and n°40278–202212051629511 v6.

Competing interests

A patent (WO2019081428A1) was previously published via the Tech Transfer Office at INSERM.

Author details

[1]Institut de Neurobiologie de la Méditerranée (INMED), Inserm, UMR1249, Parc Scientifique de Luminy, Aix-Marseille University, BP13, 13273 Marseille Cedex 09, France. [2]TAGC, INSERM, Aix Marseille University, Turing Centre for Living Systems, Marseille, France. [3]Institute of Virology, University of Ulm, Ulm, Germany. [4]CIPHE, PHENOMIN, INSERM, CNRS, Aix-Marseille University, Marseille, France. [5]DiviOmics Platform, UMS 58 BioSanD, University of Burgundy Comté, Dijon, France. [6]Present Address: Alicante Neuroscience Institute, Miguel Hernandez University, CSIC, San Juan de Alicante, Alicante, Spain. [7]Present Address: Institute for Physiology and Pathophysiology, Johannes Gutenberg University, Mainz, Germany. [8]Present Address: Argenx France SAS, 92130 Issy-Les-Moulineaux, France.

Received: 13 May 2024 Accepted: 25 October 2024
Published online: 15 November 2024

References

1. Adler SP, Nigro G. Prevention of maternal-fetal transmission of cytomegalovirus. Clin Infect Dis. 2013;57(suppl_4):S189–92. https://doi.org/10.1093/cid/cit585.
2. Leruez-Ville M, Foulon I, Pass R, Ville Y. Cytomegalovirus infection during pregnancy: state of the science. Am J Obstet Gynecol. 2020;223(3):330–49. https://doi.org/10.1016/j.ajog.2020.02.018.
3. Manicklal S, Emery VC, Lazzarotto T, Boppana SB, Gupta RK. The "silent" global burden of congenital cytomegalovirus. Clin Microbiol Rev. 2013;26(1):86–102. https://doi.org/10.1128/CMR.00062-12.
4. Børglum AD, Demontis D, Grove J, Pallesen J, Hollegaard MV, Pedersen CB, Hedemand A, Mattheisen M, Uitterlinden A, Nyegaard M, Ørntoft T, Wiuf C, Didriksen M, Nordentoft M, Nöthen MM, Rietschel M, Ophoff RA, Cichon S, Yolken RH, Mortensen PB, Mors O. Genome-wide study of association and interaction with maternal cytomegalovirus infection suggests new schizophrenia loci. Mol Psychiatry. 2014;19(3):325–33. https://doi.org/10.1038/mp.2013.2.
5. Piccirilli G, Gabrielli L, Bonasoni MP, Chiereghin A, Turello G, Borgatti EC, Simonazzi G, Felici S, Leone M, Salfi NCM, Santini D, Lazzarotto T. Fetal brain damage in human fetuses with congenital cytomegalovirus infection: histological features and viral tropism. Cell Mol Neurobiol. 2023;43(3):1385–99. https://doi.org/10.1007/s10571-022-01258-9.
6. Gabrielli L, Bonasoni MP, Lazzarotto T, Lega S, Santini D, Foschini MP, Guerra B, Baccolini F, Piccirilli G, Chiereghin A, Petrisli E, Gardini G, Lanari M, Landini MP. Histological findings in foetuses congenitally infected by cytomegalovirus. J Clin Virol. 2009;46(Suppl 4):S16-21. https://doi.org/10.1016/j.jcv.2009.09.026.
7. Sellier Y, Marliot F, Bessières B, Stirnemann J, Encha-Razavi F, Guilleminot T, Haicheur N, Pages F, Ville Y, Leruez-Ville M. Adaptive and innate immune cells in fetal human cytomegalovirus-infected brains. Microorganisms. 2020;8(2):176. https://doi.org/10.3390/microorganisms8020176.
8. Teissier N, Fallet-Bianco C, Delezoide A-L, Laquerrière A, Marcorelles P, Khung-Savatovsky S, Nardelli J, Cipriani S, Csaba Z, Picone O, Golden JA, Van Den Abbeele T, Gressens P, Adle-Biassette H. Cytomegalovirus-induced brain malformations in fetuses. J Neuropathol Exp Neurol. 2014;73(2):143–58. https://doi.org/10.1097/NEN.0000000000000038.
9. Salter MW, Stevens B. Microglia emerge as central players in brain disease. Nat Med. 2017;23(9):1018–27. https://doi.org/10.1038/nm.4397.
10. Bradford RD, Yoo Y-G, Golemac M, Pugel EP, Jonjic S, Britt WJ. Murine CMV-induced hearing loss is associated with inner ear inflammation and loss of spiral ganglia neurons. PLoS Pathog. 2015;11(4): e1004774. https://doi.org/10.1371/journal.ppat.1004774.
11. Brizić I, Hiršl L, Britt WJ, Krmpotić A, Jonjić S. Immune responses to congenital cytomegalovirus infection. Microbes Infect. 2018;20(9–10):543–51. https://doi.org/10.1016/j.micinf.2017.12.010.
12. Brizić I, Šušak B, Arapović M, Huszthy PC, Hiršl L, Kveštak D, Juranić Lisnić V, Golemac M, Pernjak Pugel E, Tomac J, Oxenius A, Britt WJ, Arapović J, Krmpotić A, Jonjić S. Brain-resident memory CD8 $^{+}$ T cells induced by congenital CMV infection prevent brain pathology and virus reactivation. Eur J Immunol. 2018;48(6):950–64. https://doi.org/10.1002/eji.201847526.
13. Kosmac K, Bantug GR, Pugel EP, Cekinovic D, Jonjic S, Britt WJ. Glucocortiocoid treatment of MCMV infected newborn mice attenuates CNS inflammation and limits deficits in cerebellar development. PLoS Pathog. 2013;9(3): e1003200. https://doi.org/10.1371/journal.ppat.1003200.
14. Kveštak D, Juranić Lisnić V, Lisnić B, Tomac J, Golemac M, Brizić I, Indenbirken D, Cokarić Brdovčak M, Bernardini G, Krstanović F, Rožmanić C, Grundhoff A, Krmpotić A, Britt WJ, Jonjić S. NK/ILC1 cells mediate neuroinflammation and brain pathology following congenital CMV infection. J Exp Med. 2021;218(5): e20201503. https://doi.org/10.1084/jem.20201503.
15. Mutnal MB, Hu S, Little MR, Lokensgard JR. Memory T cells persisting in the brain following MCMV infection induce long-term microglial activation via interferon-γ. J Neurovirol. 2011;17(5):424–37. https://doi.org/10.1007/s13365-011-0042-5.
16. Sakao-Suzuki M, Kawasaki H, Akamatsu T, Meguro S, Miyajima H, Iwashita T, Tsutsui Y, Inoue N, Kosugi I. Aberrant fetal macrophage/microglial reactions to cytomegalovirus infection. Ann Clin Transl Neurol. 2014;1(8):570–88. https://doi.org/10.1002/acn3.88.
17. Seleme MC, Kosmac K, Jonjic S, Britt WJ. Tumor necrosis factor alpha-induced recruitment of inflammatory mononuclear cells leads to inflammation and altered brain development in murine cytomegalovirus-infected newborn mice. J Virol. 2017;91(8):e01983-e2016. https://doi.org/10.1128/JVI.01983-16.
18. Slavuljica I, Kveštak D, Csaba Huszthy P, Kosmac K, Britt WJ, Jonjić S. Immunobiology of congenital cytomegalovirus infection of the central nervous system—the murine cytomegalovirus model. Cell Mol Immunol. 2015;12(2):180–91. https://doi.org/10.1038/cmi.2014.51.
19. Zhou Y-P, Mei M-J, Wang X-Z, Huang S-N, Chen L, Zhang M, Li X-Y, Qin H-B, Dong X, Cheng S, Wen L, Yang B, An X-F, He A-D, Zhang B, Zeng W-B, Li X-J, Lu Y, Li H-C, et al. A congenital CMV infection model for follow-up studies of neurodevelopmental disorders, neuroimaging abnormalities, and treatment. JCI Insight. 2022;7(1): e152551. https://doi.org/10.1172/jci.insight.152551.
20. Cloarec R, Bauer S, Luche H, Buhler E, Pallesi-Pocachard E, Salmi M, Courtens S, Massacrier A, Grenot P, Teissier N, Watrin F, Schaller F, Adle-Biassette H, Gressens P, Malissen M, Stamminger T, Streblow DN, Bruneau N, Szepetowski P. Cytomegalovirus infection of the rat developing brain in utero prominently targets immune cells and promotes early microglial activation. PLoS ONE. 2016;11(7): e0160176. https://doi.org/10.1371/journal.pone.0160176.
21. Cloarec R, Bauer S, Teissier N, Schaller F, Luche H, Courtens S, Salmi M, Pauly V, Bois E, Pallesi-Pocachard E, Buhler E, Michel FJ, Gressens P, Malissen M, Stamminger T, Streblow DN, Bruneau N, Szepetowski P. In utero administration of drugs targeting microglia improves the

neurodevelopmental outcome following cytomegalovirus infection of the rat fetal brain. Front Cell Neurosci. 2018;12:55. https://doi.org/10.3389/fncel.2018.00055.
22. Portugal CC, Socodato R, Canedo T, Silva CM, Martins T, Coreixas VSM, Loiola EC, Gess B, Röhr D, Santiago AR, Young P, Minshall RD, Paes-de-Carvalho R, Ambrósio AF, Relvas JB. Caveolin-1-mediated internalization of the vitamin C transporter SVCT2 in microglia triggers an inflammatory phenotype. Sci Signal. 2017;10(472):eaal2005. https://doi.org/10.1126/scisignal.aal2005.
23. Kannan S, Dai H, Navath RS, Balakrishnan B, Jyoti A, Janisse J, Romero R, Kannan RM. Dendrimer-based postnatal therapy for neuroinflammation and cerebral palsy in a rabbit model. Sci Transl Med. 2012. https://doi.org/10.1126/scitranslmed.3003162.
24. Niño DF, Zhou Q, Yamaguchi Y, Martin LY, Wang S, Fulton WB, Jia H, Lu P, Prindle T, Zhang F, Crawford J, Hou Z, Mori S, Chen LL, Guajardo A, Fatemi A, Pletnikov M, Kannan RM, Kannan S, et al. Cognitive impairments induced by necrotizing enterocolitis can be prevented by inhibiting microglial activation in mouse brain. Sci Transl Med. 2018;10(471):eaan0237. https://doi.org/10.1126/scitranslmed.aan0237.
25. Vane JR. Inhibition of prostaglandin synthesis as a mechanism of action for aspirin-like drugs. Nat New Biol. 1971;231(25):232–5. https://doi.org/10.1038/newbio231232a0.
26. Hagberg H, Mallard C, Ferriero DM, Vannucci SJ, Levison SW, Vexler ZS, Gressens P. The role of inflammation in perinatal brain injury. Nat Rev Neurol. 2015;11(4):192–208. https://doi.org/10.1038/nrneurol.2015.13.
27. Choi S, Langenbach R, Bosetti F. Genetic deletion or pharmacological inhibition of cyclooxygenase-1 attenuate lipopolysaccharide-induced inflammatory response and brain injury. FASEB J. 2008;22(5):1491–501. https://doi.org/10.1096/fj.07-9411com.
28. Johansson JU, Pradhan S, Lokteva LA, Woodling NS, Ko N, Brown HD, Wang Q, Loh C, Cekanaviciute E, Buckwalter M, Manning-Boğ AB, Andreasson KI. Suppression of inflammation with conditional deletion of the prostaglandin E_2 EP2 receptor in macrophages and brain microglia. J Neurosci. 2013;33(40):16016–32. https://doi.org/10.1523/JNEUROSCI.2203-13.2013.
29. Endo Y, Shoji N, Shimada Y, Kasahara E, Iikubo M, Sato T, Sasano T, Ichikawa H. Prednisolone induces microglial activation in the subnucleus caudalis of the rat trigeminal sensory complex. Cell Mol Neurobiol. 2014;34(1):95–100. https://doi.org/10.1007/s10571-013-9990-z.
30. Baca Jones CC, Kreklywich CN, Messaoudi I, Vomaske J, McCartney E, Orloff SL, Nelson JA, Streblow DN. Rat cytomegalovirus infection depletes MHC II in bone marrow derived dendritic cells. Virology. 2009;388(1):78–90. https://doi.org/10.1016/j.virol.2009.02.050.
31. Ginhoux F, Greter M, Leboeuf M, Nandi S, See P, Gokhan S, Mehler MF, Conway SJ, Ng LG, Stanley ER, Samokhvalov IM, Merad M. Fate mapping analysis reveals that adult microglia derive from primitive macrophages. Science (New York, NY). 2010;330(6005):841–5. https://doi.org/10.1126/science.1194637.
32. Babaev VR, Li L, Shah S, Fazio S, Linton MF, May JM. Combined Vitamin C and Vitamin E deficiency worsens early atherosclerosis in apolipoprotein E-deficient mice. Arterioscler Thromb Vasc Biol. 2010;30(9):1751–7. https://doi.org/10.1161/ATVBAHA.110.209502.
33. Berry A, Bellisario V, Panetta P, Raggi C, Magnifico MC, Arese M, Cirulli F. Administration of the antioxidant N-acetyl-cysteine in pregnant mice has long-term positive effects on metabolic and behavioral endpoints of male and female offspring prenatally exposed to a high-fat diet. Front Behav Neurosci. 2018;12:48. https://doi.org/10.3389/fnbeh.2018.00048.
34. Izzotti A, Balansky RM, Camoirano A, Cartiglia C, Longobardi M, Tampa E, De Flora S. Birth-related genomic and transcriptional changes in mouse lung. Mutat Res Rev Mutat Res. 2003;544(2–3):441–9. https://doi.org/10.1016/j.mrrev.2003.05.004.
35. Di Meco A, Joshi YB, Lauretti E, Praticò D. Maternal dexamethasone exposure ameliorates cognition and tau pathology in the offspring of triple transgenic AD mice. Mol Psychiatry. 2016;21(3):403–10. https://doi.org/10.1038/mp.2015.78.
36. Loux J. Antipyretic testing of aspirin in rats*1. Toxicol Appl Pharmacol. 1972;22(4):672–5. https://doi.org/10.1016/0041-008X(72)90295-5.
37. Xu X-M, Sansores-Garcia L, Chen X-M, Matijevic-Aleksic N, Du M, Wu KK. Suppression of inducible cyclooxygenase 2 gene transcription by aspirin and sodium salicylate. Proc Natl Acad Sci. 1999;96(9):5292–7. https://doi.org/10.1073/pnas.96.9.5292.
38. Colas RA, Shinohara M, Dalli J, Chiang N, Serhan CN. Identification and signature profiles for pro-resolving and inflammatory lipid mediators in human tissue. Am J Physiol Cell Physiol. 2014;307(1):C39–54. https://doi.org/10.1152/ajpcell.00024.2014.
39. Schindelin J, Arganda-Carreras I, Frise E, Kaynig V, Longair M, Pietzsch T, Preibisch S, Rueden C, Saalfeld S, Schmid B, Tinevez J-Y, White DJ, Hartenstein V, Eliceiri K, Tomancak P, Cardona A. Fiji: an open-source platform for biological-image analysis. Nat Methods. 2012;9(7):676–82. https://doi.org/10.1038/nmeth.2019.
40. Alvarez-Bolado G, Swanson LW. Developmental brain maps: structure of the embryonic rat brain. Amsterdam: Elsevier; 1996.
41. Khazipov R, Zaynutdinova D, Ogievetsky E, Valeeva G, Mitrukhina O, Manent J-B, Represa A. Atlas of the postnatal rat brain in stereotaxic coordinates. Front Neuroanat. 2015. https://doi.org/10.3389/fnana.2015.00161.
42. Di Bella DJ, Habibi E, Stickels RR, Scalia G, Brown J, Yadollahpour P, Yang SM, Abbate C, Biancalani T, Macosko EZ, Chen F, Regev A, Arlotta P. Molecular logic of cellular diversification in the mouse cerebral cortex. Nature. 2021;595(7868):554–9. https://doi.org/10.1038/s41586-021-03670-5.
43. Therneau TM, Grambsch PM. Modeling survival data: extending the cox model. New York: Springer; 2000. https://doi.org/10.1007/978-1-4757-3294-8.
44. Lenth RV. Least-squares means: the *R* Package lsmeans. J Stat Softw. 2016. https://doi.org/10.18637/jss.v069.i01.
45. Bates D, Mächler M, Bolker B, Walker S. Fitting linear mixed-effects models using lme4. J Stat Softw. 2015. https://doi.org/10.18637/jss.v067.i01.
46. Loftin CD, Tiano HF, Langenbach R. Phenotypes of the COX-deficient mice indicate physiological and pathophysiological roles for COX-1 and COX-2. Prostagland Other Lipid Mediat. 2002;68–69:177–85. https://doi.org/10.1016/S0090-6980(02)00028-X.
47. Meade EA, Smith WL, DeWitt DL. Differential inhibition of prostaglandin endoperoxide synthase (cyclooxygenase) isozymes by aspirin and other non-steroidal anti-inflammatory drugs. J Biol Chem. 1993;268(9):6610–4.
48. Sander WJ, O'Neill HG, Pohl CH. Prostaglandin E2 as a modulator of viral infections. Front Physiol. 2017. https://doi.org/10.3389/fphys.2017.00089.
49. Tam VC, Quehenberger O, Oshansky CM, Suen R, Armando AM, Treuting PM, Thomas PG, Dennis EA, Aderem A. Lipidomic profiling of influenza infection identifies mediators that induce and resolve inflammation. Cell. 2013;154(1):213–27. https://doi.org/10.1016/j.cell.2013.05.052.
50. Calvello R, Panaro MA, Carbone ML, Cianciulli A, Perrone MG, Vitale P, Malerba P, Scilimati A. Novel selective COX-1 inhibitors suppress neuroinflammatory mediators in LPS-stimulated N13 microglial cells. Pharmacol Res. 2012;65(1):137–48. https://doi.org/10.1016/j.phrs.2011.09.009.
51. Xu P, Yu Y, Wu P. Role of microglia in brain development after viral infection. Front Cell Dev Biol. 2024;12:1340308. https://doi.org/10.3389/fcell.2024.1340308.
52. Frost JL, Schafer DP. Microglia: architects of the developing nervous system. Trends Cell Biol. 2016;26(8):587–97. https://doi.org/10.1016/j.tcb.2016.02.006.
53. Thion MS, Ginhoux F, Garel S. Microglia and early brain development: an intimate journey. Science. 2018;362(6411):185–9. https://doi.org/10.1126/science.aat0474.
54. Calvello R, Lofrumento DD, Perrone MG, Cianciulli A, Salvatore R, Vitale P, De Nuccio F, Giannotti L, Nicolardi G, Panaro MA, Scilimati A. Highly selective cyclooxygenase-1 inhibitors P6 and mofezolac counteract inflammatory state both in vitro and in vivo models of neuroinflammation. Front Neurol. 2017;8:251. https://doi.org/10.3389/fneur.2017.00251.
55. Patrignani P, Dovizio M. COX-2 and EGFR: partners in crime split by aspirin. EBioMedicine. 2015;2(5):372–3. https://doi.org/10.1016/j.ebiom.2015.04.013.
56. Choi S-H, Aid S, Bosetti F. The distinct roles of cyclooxygenase-1 and -2 in neuroinflammation: implications for translational research. Trends Pharmacol Sci. 2009;30(4):174–81. https://doi.org/10.1016/j.tips.2009.01.002.
57. Zhang Y, Chen K, Sloan SA, Bennett ML, Scholze AR, O'Keeffe S, Phatnani HP, Guarnieri P, Caneda C, Ruderisch N, Deng S, Liddelow SA, Zhang C, Daneman R, Maniatis T, Barres BA, Wu JQ. An RNA-sequencing transcriptome and splicing database of glia, neurons, and vascular cells of the cerebral cortex. J Neurosci. 2014;34(36):11929–47. https://doi.org/10.1523/JNEUROSCI.1860-14.2014.

58. Mancarci BO, Toker L, Tripathy SJ, Li B, Rocco B, Sibille E, Pavlidis P. Cross-laboratory analysis of brain cell type transcriptomes with applications to interpretation of bulk tissue data. Eneuro. 2017;4(6):ENEURO.0212-17.2017. https://doi.org/10.1523/ENEURO.0212-17.2017.
59. García-Bueno B, Serrats J, Sawchenko PE. Cerebrovascular cyclooxygenase-1 expression, regulation, and role in hypothalamic-pituitary-adrenal axis activation by inflammatory stimuli. J Neurosci. 2009;29(41):12970–81. https://doi.org/10.1523/JNEUROSCI.2373-09.2009.
60. Griffin ÉW, Skelly DT, Murray CL, Cunningham C. Cyclooxygenase-1-dependent prostaglandins mediate susceptibility to systemic inflammation-induced acute cognitive dysfunction. J Neurosci. 2013;33(38):15248–58. https://doi.org/10.1523/JNEUROSCI.6361-11.2013.
61. Kapitanović Vidak H, Catela Ivković T, Vidak Z, Kapitanović S. COX-1 and COX-2 polymorphisms in susceptibility to cerebral palsy in very preterm infants. Mol Neurobiol. 2017;54(2):930–8. https://doi.org/10.1007/s12035-016-9713-9.
62. Griffin DE, Wesselingh SL, McArthur JC. Elevated central nervous system prostaglandins in human immunodeficiency virus—associated dementia. Ann Neurol. 1994;35(5):592–7. https://doi.org/10.1002/ana.410350513.
63. Zhang J, Fujii S, Wu Z, Hashioka S, Tanaka Y, Shiratsuchi A, Nakanishi Y, Nakanishi H. Involvement of COX-1 and up-regulated prostaglandin E synthases in phosphatidylserine liposome-induced prostaglandin E2 production by microglia. J Neuroimmunol. 2006;172(1–2):112–20. https://doi.org/10.1016/j.jneuroim.2005.11.008.
64. Klawonn AM, Fritz M, Castany S, Pignatelli M, Canal C, Similä F, Tejeda HA, Levinsson J, Jaarola M, Jakobsson J, Hidalgo J, Heilig M, Bonci A, Engblom D. Microglial activation elicits a negative affective state through prostaglandin-mediated modulation of striatal neurons. Immunity. 2021;54(2):225-234.e6. https://doi.org/10.1016/j.immuni.2020.12.016.
65. Zhao R, Coker OO, Wu J, Zhou Y, Zhao L, Nakatsu G, Bian X, Wei H, Chan AWH, Sung JJY, Chan FKL, El-Omar E, Yu J. Aspirin reduces colorectal tumor development in mice and gut microbes reduce its bioavailability and chemopreventive effects. Gastroenterology. 2020;159(3):969-983.e4. https://doi.org/10.1053/j.gastro.2020.05.004.
66. Thion MS, Low D, Silvin A, Chen J, Grisel P, Schulte-Schrepping J, Blecher R, Ulas T, Squarzoni P, Hoeffel G, Coulpier F, Siopi E, David FS, Scholz C, Shihui F, Lum J, Amoyo AA, Larbi A, Poidinger M, et al. Microbiome influences prenatal and adult microglia in a sex-specific manner. Cell. 2018;172(3):500-516.e16. https://doi.org/10.1016/j.cell.2017.11.042.
67. Chinery R, Beauchamp RD, Shyr Y, Kirkland SC, Coffey RJ, Morrow JD. Antioxidants reduce cyclooxygenase-2 expression, prostaglandin production, and proliferation in colorectal cancer cells. Cancer Res. 1998;58(11):2323–7.
68. Chavanas S. Peroxisome proliferator-activated receptor γ (PPARγ) activation: a key determinant of neuropathogeny during congenital infection by cytomegalovirus. Neurogenesis. 2016;3(1): e1231654. https://doi.org/10.1080/23262133.2016.1231654.
69. Layrolle P, Payoux P, Chavanas S. PPAR gamma and viral infections of the brain. Int J Mol Sci. 2021;22(16):8876. https://doi.org/10.3390/ijms22168876.
70. Vangaveti V, Baune BT, Kennedy RL. Review: hydroxyoctadecadienoic acids: novel regulators of macrophage differentiation and atherogenesis. Ther Adv Endocrinol Metab. 2010;1(2):51–60. https://doi.org/10.1177/2042018810375656.
71. Grilli M, Pizzi M, Memo M, Spano P. Neuroprotection by aspirin and sodium salicylate through blockade of NF-κB activation. Science. 1996;274(5291):1383–5. https://doi.org/10.1126/science.274.5291.1383.
72. Kopp E, Ghosh S. Inhibition of NF-κB by sodium salicylate and aspirin. Science. 1994;265(5174):956–9. https://doi.org/10.1126/science.8052854.
73. Cianferoni A, Schroeder JT, Kim J, Schmidt JW, Lichtenstein LM, Georas SN, Casolaro V. Selective inhibition of interleukin-4 gene expression in human T cells by aspirin. Blood. 2001;97(6):1742–9. https://doi.org/10.1182/blood.V97.6.1742.
74. Schrör K. Pharmacology and cellular/molecular mechanisms of action of aspirin and non-aspirin NSAIDs in colorectal cancer. Best Pract Res Clin Gastroenterol. 2011;25(4–5):473–84. https://doi.org/10.1016/j.bpg.2011.10.016.
75. Raviola S, Griffante G, Iannucci A, Chandel S, Lo Cigno I, Lacarbonara D, Caneparo V, Pasquero S, Favero F, Corà D, Trisolini E, Boldorini R, Cantaluppi V, Landolfo S, Gariglio M, De Andrea M. Human cytomegalovirus infection triggers a paracrine senescence loop in renal epithelial cells. Commun Biol. 2024;7(1):292. https://doi.org/10.1038/s42003-024-05957-5.
76. Clippinger AJ, Maguire TG, Alwine JC. Human cytomegalovirus infection maintains mTOR Activity and its perinuclear localization during amino acid deprivation. J Virol. 2011;85(18):9369–76. https://doi.org/10.1128/jvi.05102-11.
77. Nguyen LN, Kanneganti T-D. PANoptosis in viral infection: the missing puzzle piece in the cell death field. J Mol Biol. 2022;434(4): 167249. https://doi.org/10.1016/j.jmb.2021.167249.
78. Deng Y, Ostermann E, Brune W. A cytomegalovirus inflammasome inhibitor reduces proinflammatory cytokine release and pyroptosis. Nat Commun. 2024;15(1):786. https://doi.org/10.1038/s41467-024-45151-z.
79. Patel D, Roy A, Kundu M, Jana M, Luan C-H, Gonzalez FJ, Pahan K. Aspirin binds to PPARα to stimulate hippocampal plasticity and protect memory. Proc Natl Acad Sci. 2018. https://doi.org/10.1073/pnas.1802021115.
80. Pinto B, Morelli G, Rastogi M, Savardi A, Fumagalli A, Petretto A, Bartolucci M, Varea E, Catelani T, Contestabile A, Perlini LE, Cancedda L. Rescuing over-activated microglia restores cognitive performance in juvenile animals of the Dp(16) mouse model of down syndrome. Neuron. 2020;108(5):887-904.e12. https://doi.org/10.1016/j.neuron.2020.09.010.
81. El-Brolosy MA, Stainier DYR. Genetic compensation: a phenomenon in search of mechanisms. PLoS Genet. 2017;13(7): e1006780. https://doi.org/10.1371/journal.pgen.1006780.
82. Rossi A, Kontarakis Z, Gerri C, Nolte H, Hölper S, Krüger M, Stainier DYR. Genetic compensation induced by deleterious mutations but not gene knockdowns. Nature. 2015;524(7564):230–3. https://doi.org/10.1038/nature14580.
83. Morita I. Distinct functions of COX-1 and COX-2. Prostagland Other Lipid Mediat. 2002;68–69:165–75. https://doi.org/10.1016/S0090-6980(02)00029-1.
84. Hofmeyr GJ, Black RE, Rogozińska E, Heuer A, Walker N, Ashorn P, Ashorn U, Bhandari N, Bhutta ZA, Koivu A, Kumar S, Lawn JE, Munjanja S, Näsänen-Gilmore P, Ramogola-Masire D, Temmerman M, Ashorn P, Black RE, Lawn JE, et al. Evidence-based antenatal interventions to reduce the incidence of small vulnerable newborns and their associated poor outcomes. Lancet. 2023;401(10389):1733–44. https://doi.org/10.1016/S0140-6736(23)00355-0.
85. Marret S, Marchand L, Kaminski M, Larroque B, Arnaud C, Truffert P, Thirez G, Fresson J, Rozé J-C, Ancel P-Y, for the EPIPAGE Study Group. Prenatal low-dose aspirin and neurobehavioral outcomes of children born very preterm. Pediatrics. 2010;125(1):e29–34. https://doi.org/10.1542/peds.2009-0994.

Publisher's Note